



# New Calcium Carbonate Nano-particulate Pressed Powder Pellet (NFHS-2-NP) for LA-ICP-OES, LA-(MC)-ICP-MS and $\mu$ XRF

Wim Boer (1)\* , Simon Nordstad (2)\*, Michael Weber (3) , Regina Mertz-Kraus (3), Bärbel Hönisch (4), Jelle Bijma (5), Markus Raitzsch (5), Dorothee Wilhelms-Dick (5), Gavin L. Foster (6), Heather Goring-Harford (6), Dirk Nürnberg (7), Folkmar Hauff (7), Henning Kuhnert (8), Federico Lugli (9,10), Howie Spero (11), Martin Rosner (12), Piet van Gaever (1), Lennart J. de Nooijer (1) and Gert-Jan Reichart (1,13)

(1) Department of Ocean Systems, NIOZ Royal Netherlands Institute for Sea Research, Texel 1790 AB 59, The Netherlands

(2) myStandards GmbH, Kiel 24118, Germany

(3) Institute for Geosciences, Johannes Gutenberg-Universität Mainz, Mainz 55128, Germany

(4) Lamont-Doherty Earth Observatory, Department of Earth and Environmental Sciences, Columbia University, Palisades, NY, 10964, USA

(5) Alfred-Wegener-Institut, Helmholtz-Zentrum für Polar- und Meeresforschung (AWI), Bremerhaven, Germany

(6) School of Ocean and Earth Science, National Oceanography Centre Southampton, University of Southampton, Southampton, UK

(7) GEOMAR Helmholtz Centre for Ocean Research Kiel, Kiel 24148, Germany

(8) MARUM, University of Bremen, Bremen 28334, Germany

(9) Department of Chemical and Geological Sciences, University of Modena and Reggio Emilia, Via G. Campi, Modena 103 - 41125, Italy

(10) Department of Cultural Heritage, University of Bologna, Ravenna, Italy

(11) Stable Isotope Laboratory, University of California, Davis, Davis, California, USA

(12) IsoAnalysis UG, Berlin, Germany

(13) Department Earth Science, Utrecht University, Utrecht 3584 CS 8, Netherlands

\* Corresponding authors. e-mails: wim.boer@nioz.nl; nordstad@my-standards.com

A new matrix-matched reference material has been developed – NFHS-2-NP (NIOZ Foraminifera House Standard-2-Nano-Pellet) – with element mass fractions, and isotope ratios resembling that of natural foraminiferal calcium carbonate. A 180–355  $\mu\text{m}$  size fraction of planktic foraminifera was milled to nano-particles and pressed to pellets. We report reference and information values for mass fractions of forty-six elements measured by six laboratories as well as for  $^{87}\text{Sr}/^{86}\text{Sr}$  (three laboratories),  $\delta^{13}\text{C}$ ,  $\delta^{18}\text{O}$  (five laboratories) and  $^{206,207,208}\text{Pb}/^{204}\text{Pb}$  isotope ratios (one laboratory) determined by ICP-MS, ICP-OES, MC-ICP-MS, isotope ratio mass spectrometry, WD-XRF and TIMS. Inter- and intra-pellet elemental homogeneity was tested using multiple LA-ICP-MS analyses in two laboratories applying spot sizes of 60 and 70  $\mu\text{m}$ . The LA-ICP-MS results for most of the elements relevant as proxies for palaeoclimate research show RSD values < 3%, demonstrating a satisfactory homogeneous composition. Homogeneity of  $^{87}\text{Sr}/^{86}\text{Sr}$  ratios of the pellet was verified by repeated LA-MC-ICP-MS by two laboratories. Information values are reported for Pb isotope ratios and  $\delta^{13}\text{C}$ ,  $\delta^{18}\text{O}$  values. The homogeneity for these isotope systems remains to be tested by LA-MC-ICP-MS and secondary-ion mass spectrometry. Overall, our results confirm the suitability of NFHS-2-NP for calibration or monitoring the quality of *in situ* geochemical techniques.

Keywords: laser ablation, MC-ICP-MS, reference materials, carbonate, homogeneity, *in situ* techniques.

Received 23 Dec 21 – Accepted 20 Feb 22

Robust application of natural carbonates as palaeoclimate and environmental archives critically depends on accurately measured geochemical proxy signals. Elemental mass fractions, element to calcium ratios, isotope ratios or  $\delta$ -values of these carbonates are typically used in these contexts (Nürnberg *et al.* 1996, Zachos *et al.* 2001,

Hathorne *et al.* 2013). Some approaches rely on proxy data collected at micrometre-scale spatial resolution with high accuracy, for example when using bivalves (Bougeois *et al.* 2014), otoliths (Phillis *et al.* 2011, Willmes *et al.* 2016), single foraminiferal shells and/or chambers (Titelboim *et al.* 2018, Pracht *et al.* 2019), corals (Hathorne *et al.* 2011,

Tarique *et al.* 2021) or speleothems (Burns *et al.* 1998, Weber *et al.* 2021b) to reconstruct inter- or intra-annual variability of past climate. Several *in situ* state-of-the-art techniques offer excellent analytical precision and provide the desired high spatial resolution for multiple elements and/or isotope ratio measurements. Fossil biogenic carbonates have also often undergone chemical alteration during diagenesis and may carry overgrowths at their surface – whether on the outside or on the inside – that can bias the element/Ca ratio of the pristine signal (Hoogakker *et al.* 2009). Cleaning protocols have been developed for bulk analysis to remove post-depositional contaminants (e.g., Barker *et al.* 2003) but testing the effect of these cleaning methods may also benefit from accurate and precise determination of element/Ca in skeletons and shells at a high spatial resolution. Several previous studies have highlighted the need for appropriate reference materials (RMs) for these applications to ensure accuracy (e.g., Greaves *et al.* 2005, 2008, Hathorne *et al.* 2013).

Solution-based techniques generally deliver accurate and precise data via, for example, isotope dilution and standard addition methods using RMs with known chemical composition to convert measured intensities into accurate element mass fractions and isotope ratios. If the RM is of a different material than the samples, matrix effects arising from differential ionisation behaviour and interferences may bias the results (Arslan and Paulson 2002, Marchitto 2006). This can be overcome by dilution of both the digested samples and RMs with, for example, nitric acid and hence increasing the similarity in the composition of their matrices (e.g., de Villiers *et al.* 2002), or by removal of the matrix altogether with chromatography such as the commercially available seaFAST system (e.g., Arslan and Paulson 2002, Hathorne *et al.* 2012). For *in situ* techniques, such as laser ablation (multi-collector) inductively coupled plasma-mass spectrometry (LA-(MC)-ICP-MS), laser-induced breakdown spectroscopy or micro X-ray fluorescence ( $\mu$ XRF), dilution/separation is not possible and matrix effects can reduce the accuracy of the analysis. Because commonly used RMs (e.g., NIST SRM 610 and 612) are SiO<sub>2</sub> glasses with only about 8% *m/m* Ca compared with approximately 40% *m/m* Ca in carbonates, they can introduce matrix effects occurring in the laser ablation system and ICP-MS (e.g., Sylvester 2008, Jochum *et al.* 2019) when used to calibrate carbonate analyses. Although accurate results of lithophile refractory elements can be obtained using these glasses, for instance for chalcophile/siderophile elements such as Cd, Zn, Pb, P, Ni, Cu, matrix-matched calibration is recommended, and for this carbonate, RMs are preferable (Jochum *et al.* 2012). Unfortunately, previous work showed that the currently available carbonate RMs can be more heterogeneous at

the microscale than glass RMs, as demonstrated for the synthetic carbonate USGS MACS-3 (Jochum *et al.* 2019) when using small spot sizes of 55  $\mu$ m or test portions. Moreover, the large demand of such RMs may cause a shortage in terms of accessibility; for example, USGS MACS-3 is no longer commercially available, with consequences for future inter-laboratory calibrations and comparisons. The powder of coral *Porites* JCp-1 and giant clam *Tridacna gigas* JcT-1 produced by the Japanese Geological Survey (Okai *et al.* 2002, Inoue *et al.* 2004) could be pressed into pellets, but international shipping of this material is restricted by the Convention on International Trade in Endangered Species of Wild Flora and Fauna and these RMs too are not commercially available. Therefore, suitable RMs for *in situ* carbonate analysis are sparse.

In the absence of widely available solid RMs for carbonate analysis, many laboratories press their own pellets of carbonate powder. These pellets, like other existing solid RMs, are also heterogeneous at the sub-100  $\mu$ m scale. However, nano-milling is a relatively recently developed way of overcoming such homogeneity issues. Garbe-Schönberg and Müller (2014) developed a nano-milling or nano-particulate (NP) pressed powder method, which produces pellets with excellent cohesion without adding any binder. The wet milling technique results in smaller grain sizes (typically median grain size < 1.5  $\mu$ m for any material) than dry milling techniques with a minimum grain size of 5–10  $\mu$ m. Wet milling improved homogeneity substantially (Garbe-Schönberg and Müller 2014). For carbonates, this technique allows even smaller median grain size of 275 nm (S. Nordstad personal communication). Jochum *et al.* (2019) analysed MACS-3 NP, JCp-1 NP and JcT-1 NP as well as the precursor material, that is USGS MACS-3 and pellets pressed from the original powder of JCp-1 (Okai *et al.* 2002) and JcT-1 (Inoue 2007). They found that the NP pellets are more homogeneous by a factor of approximately 2–3 than the original precursor materials. The homogeneity of these NPs is similar to that of the NIST SRM 61x glasses and therefore more suitable for microanalytical purposes (Jochum *et al.* 2019).

In addition to the limited availability of matrix-matched and homogeneous RMs for mass fraction measurements, the *in situ* measurement of isotope ratios, for example, <sup>87</sup>Sr/<sup>86</sup>Sr, <sup>207,208</sup>Pb/<sup>206</sup>Pb,  $\delta^{13}$ C or  $\delta^{18}$ O in carbonates by LA-MC-ICP-MS, isotope ratio mass spectrometry (IRMS) and secondary-ion mass spectrometry (SIMS) is also hampered by the availability of suitable microanalytical RMs. For a decade, only one reported value of the <sup>87</sup>Sr/<sup>86</sup>Sr ratio (Ohno and Hirata 2007) was available for the original

powder JCI-1, but recently this has been complemented by measurements using multiple techniques in different laboratories (Weber *et al.* 2018) to establish a robust Sr isotope ratio for this RM. In particular, there is a limited availability of RMs matching the sample mass fraction of interest. Recently, Weber *et al.* (2020a) presented a new synthetic carbonate nanopowder RM called NanoSr, with an Sr mass fraction of  $\sim 500 \mu\text{g g}^{-1}$  for *in situ* Sr isotope measurements. Furthermore, a new RM (GBW04481) for calcite oxygen and carbon isotopic microanalysis has been developed with  $\delta^{18}\text{O}_{\text{VPDB}} = -23.12 \pm 0.15\text{‰}$  (1s) and  $\delta^{13}\text{C}_{\text{VPDB}} = -5.23 \pm 0.06\text{‰}$  (1s) for the Oka calcite (Tang *et al.* 2019). Availability of such well-characterised, high-quality carbonate RM is a prerequisite for high-precision SIMS O and C isotopic microanalysis (Tang *et al.* 2019).

In element determinations using solution measurements, calibration curves are often used with multiple RMs with a range of element mass fractions. *In situ* techniques often use a single RM for calibration. A disadvantage of this strategy is the lack of control on linearity across a range of element mass fractions and the assumption that the calibration line passes through the origin, which is not the case for an interfered element. Hence, accuracy of LA-ICP-MS could be increased with the same calibration strategies as solution measurements, if more suitable carbonate RMs were available. Despite the finding that using the NIST SRM 61X series glasses can yield accurate results when calibrating measurements of carbonates by LA-ICP-MS (e.g. Jochum *et al.* 2012), it would be preferable to use – in addition – homogeneous carbonate RMs such as JCI-1 NP, JCI-1 NP, MACS-3 NP and for instance the new RM NFHS-2-NP presented herein.

To improve the limited availability of matrix-matched RMs for element mass fraction and isotope ratios for *in situ* techniques, we present a new carbonate RM NFHS-2-NP (NIOZ Foraminifera House Standard-2-Nano-Pellet) made from a nano-milled (Garbe-Schönberg and Müller 2014) mixed assemblage of planktic foraminifera. In this study, we present an inter-laboratory compilation of data from solution ICP-MS, ICP-OES, LA-ICP-(MC)-MS, XRF, bulk analyses of forty-six element mass fractions (including elements relevant for environmental research such as B, Ba, Mg, Mn, Na, Sr) as well as isotope ratios ( $^{87}\text{Sr}/^{86}\text{Sr}$ ,  $^{206}\text{Pb}/^{208}\text{Pb}$ ,  $^{204}\text{Pb}$ ,  $\delta^{13}\text{C}$ ,  $\delta^{18}\text{O}$ ), to establish the composition and verify the homogeneity of the NFHS-2-NP pellets. Seven laboratories contributed data for element mass fractions, five laboratories for  $\delta^{13}\text{C}$  and  $\delta^{18}\text{O}$ , four laboratories for  $^{87}\text{Sr}/^{86}\text{Sr}$  ratios and one laboratory for Pb isotopes.

## Materials and methods

### NFHS-2-NP (NIOZ foraminifera house standard-2-nano-pellet)

NFHS-2-NP (Figure 1) was prepared from a mixed assemblage of planktic foraminifera shells, sieved from a calcareous ooze collected in section#1 (5.3–6.5 m) of a piston core (PE174-15PC) and retrieved by the Royal Netherlands Institute for Sea Research (NIOZ) from Walvis Ridge (2878 m water depth; 29°85S, 2°3405E). The sediments were wet sieved over 63, 180 and 355  $\mu\text{m}$  mesh sizes. The 180–355  $\mu\text{m}$  size fraction was subsequently cleaned according to the protocol of Barker *et al.* (2003) and scaled up to clean  $\sim 300$  g of material. The cleaned material was pre-milled with a Retsch Planetary Ball Mill PM 100 using cleaned zirconium oxide beakers. The, at this stage obtained, powder NFHS1 has been used as an in-house RM for  $\delta^{13}\text{C}$ ,  $\delta^{18}\text{O}$  and solution ICP-MS measurements since 2014. To improve the homogeneity of pellets for LA-ICP-MS measurements, NFHS1 powder was subsequently wet-milled using agate milling gear by myStandards GmbH (Kiel, Germany) to produce nano-particles. Using a programmable hydraulic press, these particles were then pressed to a pellet (Figure 1) with a diameter of 5 mm (4 tons) or 13 mm (10 tons). A binder was not added.

### Analytical techniques

In this study, twelve laboratories were involved in the characterisation process for NFHS-2-NP (Table 1). Seven laboratories were involved in the determination of trace, minor and major elements, five in the determination of stable isotopes, four determined strontium isotopes, and one laboratory determined Pb isotopes. Data resulting from TIMS, MC-ICP-MS, sector field (SF)-ICP-MS, Q-ICP-MS, triple quadrupole (QQQ)-ICP-MS, ICP-OES, LA-MC-ICP-MS, LA-Q-ICP-MS, XRF and KIEL-IRMS measurements are presented and discussed. In the following, analytical procedures and most important features of the instruments used in this study are described.

### Elemental mass fractions

Mass fractions of the powder of NFHS-2-NP were determined for forty-six elements (Al, B, Ba, Cd, Ce, Co, Cr, Cs, Cu, Dy, Er, Eu, Fe, Ga, Gd, Hf, Ho, K, La, Li, Lu, Mg, Mn, Na, Nd, Ni, P, Pb, Pr, Rb, S, Sc, Si, Sm, Sn, Sr, Tb, Th, Ti, Tm, V, U, Y, Yb, Zn and Zr) by AWI, LDEO, NIOZ, University of Southampton and two anonymous laboratories (Labs 5 and 6) using SF-ICP-MS, quadrupole-ICP-MS and ICP-OES after  $\text{HNO}_3/\text{HF}$ ,  $\text{HNO}_3/\text{HF}/\text{HCl}$ ,  $\text{HNO}_3/\text{HF}/\text{HClO}_4$  or  $\text{HNO}_3$



**Figure 1. Photograph of a nano-milled pellet (blue arrow) made from a mixed assemblage of planktic foraminifera (in front of pellet) from the 180–355  $\mu\text{m}$  size fraction of a piston core from Walvis Ridge in the South Atlantic Ocean. Photograph by Ellen R. Pruiksma.**

digestion. At Lab 6, the powder was analysed by WD-XRF in addition to ICP-OES and QQQ-ICP-MS. Participants were asked to not clean the samples again before analysis, but to analyse them as provided.

At AWI (Lab 1A), a sub-sample (~ 5 mg) of the NFHS-2-NP powder was dissolved in double-distilled 1 mol l<sup>-1</sup> HNO<sub>3</sub>, from which a small aliquot was diluted with double-distilled 0.3 mol l<sup>-1</sup> HNO<sub>3</sub> to achieve a target [Ca] of ~ 10  $\mu\text{g g}^{-1}$ . The sample measurements were bracketed by measurements of a five-point calibration block made from an in-house artificial foraminiferal RM. A solution of JcP-1 was analysed along with the sample as a quality control to ensure the accuracy of the measurements. The liquids were introduced into a Nu Instruments Atom high-resolution ICP-MS via a Savilleux PFA nebuliser (self-aspirating at ~ 100  $\mu\text{l min}^{-1}$ ) and an ESI quartz cyclonic spray chamber. The RMs and samples were analysed twice in quintuplicate for the isotopes <sup>7</sup>Li, <sup>11</sup>B, <sup>25</sup>Mg, <sup>27</sup>Al, <sup>43</sup>Ca, <sup>51</sup>V, <sup>87</sup>Sr, <sup>111</sup>Cd, <sup>137</sup>Ba, <sup>146</sup>Nd and <sup>238</sup>U in low-resolution mode. From the ten

measurements in total of the NFHS-2-NP, the mean concentrations and repeatability are reported.

At LDEO (Lab 2), cleaned carbonate samples were dissolved in 2% HNO<sub>3</sub> and analysed for [Ca] and element/Ca ratios on a Thermo Scientific iCAP-Q Q-ICP-MS. First, a small aliquot (10–20%) of this solution was used to determine [Ca]. Upon [Ca] determination, each sample solution was diluted to 50  $\mu\text{g g}^{-1}$  Ca. Signal intensities of trace elements were then measured using a Thermo Scientific iCAP Q ICP-MS following methods adapted from Yu *et al.* (2005). Signals of low-mass isotopes <sup>11</sup>B were measured in standard mode; <sup>23</sup>Na, <sup>27</sup>Al, <sup>43</sup>Ca, <sup>55</sup>Mn, <sup>56</sup>Fe and <sup>111</sup>Cd were measured in kinetic energy discrimination mode using a He collision cell to minimise polyatomic interferences. To minimise matrix effects and to account for instrumental drift, signal intensities were corrected with an internal multi-element quality control reference solution (containing 50  $\mu\text{g g}^{-1}$  Ca) measured every ten samples. Concentrations and element ratios (relative to Ca) were calculated from signal intensities measured on a multi-element stock solution prepared gravimetrically from trace element-grade stock solutions. These reference solutions contained 50  $\mu\text{g g}^{-1}$  Ca and were prepared with a range of trace element concentrations reflective of typical foraminiferal samples (e.g., Mg/Ca between 0.5 and 5.5 mmol mol<sup>-1</sup>), creating calibrations of element intensity to concentration.

At NIOZ (Lab 3A), a 20 mg test portion of oven-dried (110 °C for 2 h) powder of NFHS-2-NP ( $n = 5$ ) was weighed on a six-decimal balance and was digested in 4 ml PTFE rocket beakers after a total digestion procedure using concentrated ultrapure HNO<sub>3</sub>/HF/HCl (Durand *et al.* 2016), adjusted to a mass of 20 mg of the RM. After removal of the HNO<sub>3</sub>/HF/HCl matrix in a class 5 flow bench in a class 7 cleanroom, the digested RM was dissolved in ultrapure 0.1 mol l<sup>-1</sup> HNO<sub>3</sub> prepared with low boron ultrapure water (resistivity > 18.2 M $\Omega$  cm). In addition to the total digestion and for comparison, the NFHS-2-NP ( $n = 2$ ) was dissolved in ultrapure 0.1 mol l<sup>-1</sup> HNO<sub>3</sub>. To determine the [Ca] and element/Ca ratios in the digested RM, a SF-ICP-MS instrument was used (Thermo Fischer Scientific Element-2). For the [Ca] determination, intensities of masses <sup>44</sup>Ca, <sup>45</sup>Sc and <sup>87</sup>Sr<sup>2+</sup>, <sup>87</sup>Sr and <sup>88</sup>Sr were measured in medium resolution. The intensity of <sup>44</sup>Ca was corrected for an <sup>88</sup>Sr<sup>2+</sup> interference (Sr<sup>2+</sup>/Sr<sup>+</sup> was 1.4%). <sup>45</sup>Sc was used as an internal standard element to correct for drift during the measurement. Accordingly, to these [Ca], solution of NFHS-2-NP was diluted to obtain 100  $\mu\text{g g}^{-1}$  Ca. We measured samples in replicate by monitoring the isotopes <sup>7</sup>Li, <sup>11</sup>B, <sup>23</sup>Na, <sup>25</sup>Mg, <sup>43</sup>Ca, <sup>66</sup>Zn,

**Table 1.**  
**Institutions involved in the characterisation process of NFHS-2-NP**

Lab ID	Technique	Analyte	Institution	Acronym	Comment
1A	SF-ICP-MS	Trace elements	Alfred-Wegener-Institut, Helmholtz-Zentrum für Polar- und Meeresforschung, DE	AWI	
1B	KIEL/IRMS	$\delta^{13}\text{C}$ , $\delta^{18}\text{O}$	Lamont-Doherty Earth Observatory and Columbia University, USA	LDEO	
2	Q-ICP-MS	Trace elements	Royal Netherlands Institute for Sea Research, NL	NIOZ	
3A	SF-ICP-MS	Trace elements	School of Ocean and Earth Science, University of Southampton, National Oceanography Centre Southampton	Southampton	
3B	LA-Q-ICP-MS	Trace elements			
3C	KIEL/IRMS	$\delta^{13}\text{C}$ , $\delta^{18}\text{O}$			
4	ICP-MS	Trace elements			
5	ICP-OES/Q-ICP-MS	Trace elements	Anonymous		Accredited in accordance with ISO 17025
6A	ICP-OES	Major- and trace elements	Anonymous		Accredited in accordance with ISO 17025
6B	QQQ-ICP-MS	Major- and trace elements			
6C	fusion XRF	Major- and trace elements			
7A	LA-Q-ICP-MS	Trace element	Institute for Geosciences, Johannes Gutenberg-Universität, Mainz, DE	JGU	
7B	MC-ICP-MS	Sr isotopes			
7C	LA-MC-ICP-MS	Sr isotopes			
8	TIMS	Sr isotopes	IsoAnalysis UG, Berlin, DE	IsoAnalysis	Accredited in accordance with ISO 17025
9A	TIMS	Sr, Pb isotopes	GEOMAR Helmholtz Centre for Ocean Research Kiel, DE	GEOMAR	
9B	KIEL/IRMS	$\delta^{13}\text{C}$ , $\delta^{18}\text{O}$			
10	LA-MC-ICP-MS	Sr isotopes	Geochemistry Lab, University of Modena and Reggio Emilia, IT	Modena	
11	KIEL/IRMS	$\delta^{13}\text{C}$ , $\delta^{18}\text{O}$	MARUM, University of Bremen, DE	Marum	
12	KIEL/IRMS	$\delta^{13}\text{C}$ , $\delta^{18}\text{O}$	Stable Isotope Laboratory, UC Davis, US	Davis	

$^{85}\text{Rb}$ ,  $^{87}\text{Sr}$ ,  $^{88}\text{Sr}$ ,  $^{112}\text{Cd}$ ,  $^{121}\text{Sb}$ ,  $^{138}\text{Ba}$ ,  $^{208}\text{Pb}$  and  $^{238}\text{U}$  in low resolution, the isotopes  $^{27}\text{Al}$ ,  $^{31}\text{P}$ ,  $^{32}\text{S}$ ,  $^{43}\text{Ca}$ ,  $^{51}\text{V}$ ,  $^{52}\text{C}$ ,  $^{55}\text{Mn}$ ,  $^{56}\text{Fe}$ ,  $^{59}\text{Co}$ ,  $^{60}\text{Ni}$  and  $^{63}\text{Cu}$  in medium resolution and the isotopes  $^{39}\text{K}$ ,  $^{43}\text{Ca}$  and  $^{75}\text{As}$  in high resolution. To determine element/Ca ( $\text{mmol mol}^{-1}$ ) ratios, we used a ratio calibration method (de Villiers *et al.* 2002) with all RMs, QCMs JCP-1 and JCT-1, drift monitor materials and six calibration materials having a similar matrix of  $100 \pm 5 \mu\text{g g}^{-1}$  Ca in  $0.1 \text{ mol l}^{-1}$   $\text{HNO}_3$ .

At the University of Southampton (Lab 4), a 75 mg sub-sample of the RM was dissolved in an acid-washed PFA vial with 5 ml of  $0.5 \text{ mol l}^{-1}$   $\text{HNO}_3$  that was prepared using thermally distilled  $\text{HNO}_3$  and low boron high-purity (Milli-Q) water. Following Henahan *et al.* (2015), measurement of element/Ca ratios was performed with a Thermo Scientific Element II SF-ICP-MS with a PTFE barrel spray chamber introduction system, into which ammonia gas was added to aid the washout of

boron (Al-Ammar *et al.* 2000). Standards and samples were signal-matched at  $1 \text{ mmol l}^{-1}$  Ca, and a standard bracketing technique was employed to correct mass bias drift within the run, using an in-house multi-element standard, which was measured between every three samples/standards. All isotopes ( $^7\text{Li}$ ,  $^{11}\text{B}$ ,  $^{23}\text{Na}$ ,  $^{24}\text{Mg}$ ,  $^{25}\text{Mg}$ ,  $^{27}\text{Al}$ ,  $^{43}\text{Ca}$ ,  $^{48}\text{Ca}$ ,  $^{55}\text{Mn}$ ,  $^{86}\text{Sr}$ ,  $^{87}\text{Sr}$ ,  $^{111}\text{Cd}$ ,  $^{138}\text{Ba}$ ,  $^{146}\text{Nd}$ ,  $^{238}\text{U}$  and  $^{56}\text{Fe}$ ) were measured in low-resolution mode except for  $^{56}\text{Fe}$ , which was measured in medium resolution. Isobaric interferences from doubly charged  $^{48}\text{Ca}$  on  $^{24}\text{Mg}$  and  $^{86}\text{Sr}$  on  $^{43}\text{Ca}$  were corrected using measurements of doubly charged  $^{43}\text{Ca}$  and  $^{87}\text{Sr}$  respectively. In-house consistency RMs with varying mass fractions of elements relative to Ca were used to check the validity of the determination. Five analyses of the RM were made during the measurement session, and the repeatability (RSD) was better than 2% for all element/Ca ratios except for those involving  $^{11}\text{B}$ ,  $^{56}\text{Fe}$ ,  $^{111}\text{Cd}$  and  $^{238}\text{U}$ , which were better than 4%.



At Lab 5, 250 mg of sample ( $n = 5$ ) was dissolved in perchloric ( $\text{HClO}_4$ ), nitric ( $\text{HNO}_3$ ), hydrochloric ( $\text{HCl}$ ) and hydrofluoric acid ( $\text{HF}$ ). The remaining residue after drying was dissolved with dilute  $\text{HCl}$  and analysed by ICP-MS and ICP-OES. Results were corrected for spectral and inter-element interferences. Further information was omitted.

At Lab 6, the powder was analysed by WD-XRF as a fused bead after lithium borate fusion as well as by QQQ-ICP-MS and ICP-OES after *aqua regia* ( $\text{HNO}_3 + \text{HCl}$ , 1 to 3 ratio) and four-acid (see ALS) digestion. Sample masses for XRF, *aqua regia* and four-acid were 1, 1 g and 250 mg respectively. Further information was omitted.

The participants reported their data either as element to calcium ratios ( $\mu\text{mol mol}^{-1} \text{Ca}$  or  $\text{mmol mol}^{-1} \text{Ca}$ ) obtained by an intensity ratio calibration method (e.g., de Villiers *et al.* 2002) or as mass fractions (%  $m/m$  or  $\mu\text{g g}^{-1}$ ). To allow better intercomparison of the data, we used the mean  $[\text{Ca}]$  of  $38.5 \pm 0.6\% m/m$  ( $\text{CaO } 53.9 \pm 0.9\% m/m$ ) determined after a three-acid total digestion by SF-ICP-MS (NIOZ), after a four-acid total digestion by ICP-OES (Lab 6B) and XRF (Lab 6C). This value was subsequently used to convert element ratios into element mass fractions, which we report throughout the remainder of the manuscript.

### Element mass fraction homogeneity

Testing for elemental homogeneity was done according to ASTM Guide E826-14 by dividing the surface of the test pellets into distinct zones (Figure 2; ASTM Guide E826-14, 2014). Analyses were performed at NIOZ (Lab 3B) and JGU (Lab 7A). Operation parameters are provided in Table 2.

The larger the spot size, the more material and potential inhomogeneities are averaged (Jochum *et al.* 2012). To minimise such adverse smoothing, spot sizes of 60 and 70  $\mu\text{m}$  were chosen.

At NIOZ (Lab 3B), four pellets of NFHS-2-NP were analysed with  $7 \times 3$  spots programmed on every pellet in the pattern shown in Figure 2. The distance between the three spots that were close to each cluster was around 200  $\mu\text{m}$ . Spots were measured in a random order to avoid systematic offsets. Ablation was performed with helium as carrier gas and mixed with argon before entering the ICP-MS. A self-made squid following the design of Eggins *et al.* (1998) was used to produce a more stable signal. Two interface vacuum pumps were used to increase the sensitivity. Backgrounds were measured for 40 s and ablation time was 40 s, followed by 5 s of wash out. Data reduction was performed using an adapted version of the data reduction

software SILLS (Signal Integration for Laboratory Laser Systems, Guillon *et al.* 2008) in Matlab. Data from the first 5 s of every laser ablation profile were excluded to avoid potential surface contamination. To calculate element mass fractions, relative sensitivity factors using  $^{43}\text{Ca}$  as an internal standard element were calculated using both NIST SRM 610 and NIST SRM 612 as calibrants using the reference values reported in the GeoReM database (Jochum *et al.* 2005, 2011). The intensity of  $^{43}\text{Ca}$  was corrected for an  $^{86}\text{Sr}^{2+}$  interference ( $\text{Sr}^{2+}/\text{Sr}^+$  was 0.39%). QCMs JCp-1 NP ( $n = 21$ ), JCI-1 NP ( $n = 21$ ), ECRM752 NP ( $n = 21$ ), RS3 NP ( $n = 21$ ) and MACS-3 ( $n = 24$ ) were measured in the same sequence to monitor precision and accuracy of the applied protocol. JCp-1 NP made by myStandards GmbH was used to quantify drift and was measured in triplicate after every seventh sample.

At JGU (Lab 7B), one pellet was analysed with  $7 \times 3$  patterns (repeated three times) as shown in Figure 2. Ablation was carried out under a He atmosphere and the sample gas was mixed with Ar before entering the plasma. Backgrounds were measured for 20 s prior to each ablation. Ablation time was 40 s, followed by 20 s of wash out. Signals were recorded in time-resolved mode and processed using an in-house Excel spreadsheet (Jochum *et al.* 2007). Details of the calculations are given in Mischel *et al.* (2017). NIST SRM 610 and 612 were used as calibration materials, applying the reference values reported in the

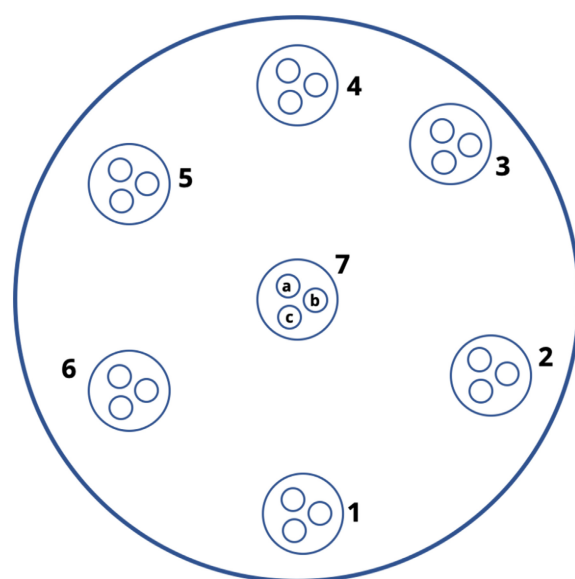


**Figure 2. Laser ablation spots (7 times 3) used for testing homogeneity. Letters a, b, c are only shown in section 7 as an example and omitted in the other sections for image clarity.**

**Table 2.**  
Operating parameters LA-Q-ICP-MS at NIOZ and JGU

	<b>NIOZ</b>	<b>JGU</b>
<b>Laser ablation system</b>	<b>ESI NWR193UC</b>	<b>ESI NWR193</b>
<b>Sample cell</b>	<b>Two-Vol2</b>	<b>Two-Vol2</b>
Wavelength	193 nm	193 nm
Pulse duration	4 ns	4 ns
Laser fluence	3 J cm <sup>-2</sup>	3 J cm <sup>-2</sup>
Laser spot size	60 μm	70 μm
Laser repetition rate	10 Hz	10 Hz
Carrier gas flow rate (He)	0.6 l min <sup>-1</sup>	0.7 l min <sup>-1</sup>
Ablation time	40 s	40 s
<b>ICP-MS</b>	<b>Thermo Fisher Scientific iCAP-Q</b>	<b>Agilent 7500ce</b>
Measuring mode	Standard (no collision gas)	Standard (no collision gas)
Cooling gas flow rate	17.5 l min <sup>-1</sup>	15 l min <sup>-1</sup>
RF power	1550 W	1200 W
Auxiliary gas flow rate	0.75 l min <sup>-1</sup>	1 l min <sup>-1</sup>
Sample gas flow rate (Ar)	0.45 l min <sup>-1</sup>	0.8 l min <sup>-1</sup>
Monitored isotopes	<sup>11</sup> B, <sup>23</sup> Na, <sup>25</sup> Mg, <sup>27</sup> Al, <sup>29</sup> Si, <sup>43</sup> Ca, <sup>55</sup> Mn, <sup>57</sup> Fe, <sup>66</sup> Zn, <sup>88</sup> Sr, <sup>89</sup> Y, <sup>137</sup> Ba, <sup>208</sup> Pb, <sup>238</sup> U	<sup>7</sup> Li, <sup>9</sup> Be, <sup>11</sup> B, <sup>23</sup> Na, <sup>25</sup> Mg, <sup>27</sup> Al, <sup>29</sup> Si, <sup>31</sup> P, <sup>39</sup> K, <sup>43</sup> Ca, <sup>45</sup> Sc, <sup>47</sup> Ti, <sup>49</sup> Ti, <sup>51</sup> V, <sup>53</sup> Cr, <sup>55</sup> Mn, <sup>56</sup> Fe, <sup>57</sup> Fe, <sup>59</sup> Co, <sup>60</sup> Ni, <sup>63</sup> Cu, <sup>65</sup> Cu, <sup>66</sup> Zn, <sup>67</sup> Zn, <sup>71</sup> Ga, <sup>75</sup> As, <sup>85</sup> Rb, <sup>86</sup> Sr, <sup>88</sup> Sr, <sup>89</sup> Y, <sup>90</sup> Zr, <sup>93</sup> Nb, <sup>98</sup> Mo, <sup>111</sup> Cd, <sup>118</sup> Sn, <sup>133</sup> Cs, <sup>135</sup> Ba, <sup>137</sup> Ba, <sup>139</sup> La, <sup>140</sup> Ce, <sup>141</sup> Pr, <sup>143</sup> Nd, <sup>147</sup> Sm, <sup>153</sup> Eu, <sup>157</sup> Gd, <sup>159</sup> Tb, <sup>163</sup> Dy, <sup>165</sup> Ho, <sup>167</sup> Er, <sup>169</sup> Tm, <sup>173</sup> Yb, <sup>175</sup> Lu, <sup>177</sup> Hf, <sup>184</sup> W, <sup>208</sup> Pb, <sup>232</sup> Th, <sup>238</sup> U
Integration time	0.01 s all, but <sup>11</sup> B (0.1 s), <sup>25</sup> Mg (0.02 s) and <sup>57</sup> Fe (0.02 s)	0.01 s
Time per pass	280 ms	660 ms
ThO/Th	0.6%	0.4%
U/Th	1.06	1.1
Lab ID.	3B	7A

GeoReM database (<http://georem.mpch-mainz.gwdg.de/>, Application Version 27, Jochum *et al.* 2005, 2011) to calculate the element concentrations of the sample measurements. During each run, USGS BCR-2G (basalt), USGS MACS-3 (synthetic carbonate) and JCp-1 NP and JcT-1 NP (biogenic carbonates) were analysed repeatedly as QCMs to monitor precision and accuracy of the measurements as well as the calibration strategy. All RMs were analysed at the beginning and at the end of a sequence and after twenty-one spots on the samples. For all materials <sup>43</sup>Ca was used as the internal standard element, applying to NFHS-2-NP, the preferred values reported in the GeoReM database for NIST SRM 610 and 612, the QCMs USGS BCR-2G and MACS-3 and for JCp-1 and JcT-1 (values provided by Okai *et al.* (2002) and Aizawa (2008) respectively). Resulting element mass fractions for the QCMs agreed typically within uncertainties with published values.

### <sup>87</sup>Sr/<sup>86</sup>Sr isotope ratios

Strontium isotope ratios of the powder were measured by three different laboratories (IsoAnalysis UG, GEOMAR, JGU) using TIMS and MC-ICP-MS.

At JGU (Lab 7B), the solution-based <sup>87</sup>Sr/<sup>86</sup>Sr ratios were obtained by coupling the Thermo Neptune Plus MC-ICP-MS with an ESI Apex Omega HF desolvator system, following the methods described in Weber *et al.* (2020b). Prior to analysis, about 8 mg of NFHS-2-NP was dissolved in 5 ml of 3 mol l<sup>-1</sup> HNO<sub>3</sub> in a closed PFA beaker overnight on a hot plate at 120 °C. Ten aliquots of 300 μl from the digested material were processed together with a modern seashell following the methods described in Lugli *et al.* (2020) and Weber *et al.* (2018). All solutions were prepared at 10 ng g<sup>-1</sup> Sr in 0.8 mol l<sup>-1</sup> HNO<sub>3</sub> and analysed in a standard sample bracketing sequence using NIST SRM 987 for bracketing and normalisation to <sup>87</sup>Sr/<sup>86</sup>Sr = 0.710248. Within the same measurement session, NIST SRM 987 yielded a mean <sup>87</sup>Sr/<sup>86</sup>Sr of 0.71026 ± 0.00003 (2s, n = 57). The modern seashell yielded an <sup>87</sup>Sr/<sup>86</sup>Sr of 0.70917 ± 0.00001 (2SE, n = 1). Data evaluation at JGU was performed offline, using an in-house R script (R Core Team 2020).

At IsoAnalysis UG (Lab 8), sample test portions of about 60 mg were dissolved in 6 mol l<sup>-1</sup> HNO<sub>3</sub>, using PFA vials, at 120 °C. Strontium was separated by ion chromatography

(Eichrom® Sr-Spec resin) and determined from three separate aliquots sevenfold using TIMS. The raw data were converted using an  $^{86}\text{Sr}/^{88}\text{Sr}$  ratio of 0.1194 and a best practice value of 0.71025 for NIST SRM 987. Rubidium was measured on mass 85, and the data were corrected for a potential proportion of  $^{87}\text{Rb}$ .

At GEOMAR (Lab 9A), about 100 mg of NFHS-2-NP was dissolved in 3 ml of 6 mol l<sup>-1</sup> HCl at 100 °C overnight in closed 7 ml Savillex® PTFE beakers. Samples beakers were then opened, and samples dried at 110 °C. Strontium separation used a single pass through BioRad Micro Bio-Spin™ columns filled with ~ 150 µl of Eichrom® Sr-Spec resin (50–100 µm) equilibrated in 6 mol l<sup>-1</sup> HNO<sub>3</sub>. Strontium was cleaned by fivefold addition of 500 µl increments of 6 mol l<sup>-1</sup> HNO<sub>3</sub> followed by a final washout with 2 ml 0.05 mol l<sup>-1</sup> HNO<sub>3</sub>. USGS BCR-2 (~ 100 mg) QCM, leached in 2 mol l<sup>-1</sup> HCl at 70 °C prior to dissolution, was routinely processed along with NFHS-2-NP but followed the silicate digestion procedure outlined in Hoernle *et al.* (2008). Strontium isotope ratios were determined on a Thermo Scientific® TRITON Plus TIMS operating multi-dynamic mode for Sr. Within run mass bias correction uses  $^{86}\text{Sr}/^{88}\text{Sr} = 0.1194$ . Possible mass interference of  $^{87}\text{Rb}$  on  $^{87}\text{Sr}$  was monitored by the  $^{85}\text{Rb}$  signal, but none was detected in any of the measurements. RM NIST SRM 987 (Sr) was repeatedly measured along with the samples and gave  $^{87}\text{Sr}/^{86}\text{Sr} = 0.710262 \pm 0.000007$  (2s,  $n = 8$ ). The laboratory routinely reports sample data relative to  $^{87}\text{Sr}/^{86}\text{Sr} = 0.710250$  for NIST SRM 987 with an intermediate measurement precision of  $\pm 0.000009$  (2s,  $n = 834$  since 2014). Total chemistry blanks were < 100 pg Sr and therefore considered negligible relative to the amounts of sample used. Leached RM USGS BCR-2 gave  $^{87}\text{Sr}/^{86}\text{Sr} = 0.705001 \pm 0.000005$  (2SE) and lies within those of Fourny *et al.* (2016) for unleached USGS BCR-2.

Spatial homogeneity was tested by LA-MC-ICP-MS in two laboratories (JGU and Modena). JGU (Lab 7C) used a line scan with circular spot of 70 µm and line length of 500 µm ( $n = 21$ ). Modena (Lab 10) employed two different sampling strategies: line scans with circular spot of 100 µm and a line length of 600 µm ( $n = 12$ ), and spot scans with a size of 80 µm and a dwell time of 50 s ( $n = 3$ ). Operation parameters are provided in Table 3.

At Modena (Lab 10), analyses were performed using a NewWave UP 213 nm laser ablation system, coupled to a Neptune MC-ICP-MS, following Lugli *et al.* (2020) and Weber *et al.* (2018). Potential interferences of Kr on the isotopes of interest were corrected by subtracting the on-peak baseline acquired during the laser warm-up (~ 30–60 s). To

**Table 3.**  
**Operating parameters LA-MC-ICP-MS at Modena and JGU**

Laser ablation system	JGU	Modena
	ESI NWR193	New Wave UP 213
Sample cell	Two-Vol <sup>2</sup>	Single volume
Wavelength	193 nm	213 nm
Pulse duration	4 ns	4 ns
Laser fluence	5 J cm <sup>-2</sup>	10 J cm <sup>-2</sup>
Spot size — line scans	70 µm	100 µm
Line length	500 µm	600 µm
Spot size — depth profiling	N/A	80 µm
Laser repetition rate	10 Hz	10 Hz
Carrier gas flow rate (He)	0.8 l min <sup>-1</sup>	0.6 l min <sup>-1</sup>
Ablation time	100 s	Spots 50 s, Lines 120 s
<b>ICP-MS</b>	<b>Thermo Neptune plus</b>	<b>Thermo Neptune</b>
Resolution	Low	Low
Cooling gas flow rate	15 l min <sup>-1</sup>	15 l min <sup>-1</sup>
RF power	1200 W	1200 W
Auxiliary gas flow rate	0.7 l min <sup>-1</sup>	0.8 l min <sup>-1</sup>
Sample gas flow rate (Ar)	0.9 l min <sup>-1</sup>	1 l min <sup>-1</sup>
Lab ID.	7C	10

correct for the presence of isobaric Rb on  $m/z$  87, the  $^{85}\text{Rb}$  was measured and an  $^{87}\text{Rb}/^{85}\text{Rb}$  ratio of 0.3856656 was used. Mass bias normalisation of Rb and Sr was performed using the exponential law and a stable  $^{88}\text{Sr}/^{86}\text{Sr}$  ratio of 8.375209 (Berglund and Wieser 2011). Rare-earth element and Ca dimers/argides were monitored, but not corrected because their interference with the analyses was negligible. A modern seashell (*Acanthocardia* sp., Adriatic Sea; expected seawater  $^{87}\text{Sr}/^{86}\text{Sr}$  ratio: ~ 0.70917 from, for example Palmer and Edmond 1992) and the NanoSr RM (Weber *et al.* 2020a reference  $^{87}\text{Sr}/^{86}\text{Sr}$  ratio:  $0.70756 \pm 0.00003$ ) were also analysed during the session, yielding an  $^{87}\text{Sr}/^{86}\text{Sr}$  ratio of  $0.70918 \pm 0.00002$  (2s,  $n = 5$ ) and of  $0.70753 \pm 0.00001$  (2s,  $n = 2$ ) respectively.

At JGU (Lab 7C), a Neptune Plus (Thermo Scientific) MC-ICP-MS was coupled to an ArF Excimer 193 nm laser ablation system (ESI NWR193) with a TwoVol<sup>2</sup> ablation cell. To introduce N<sub>2</sub> and thereby enhance sensitivity, a CETAC Aridus 3 desolvating system was coupled to the sample line (Weber *et al.* 2020b). The analytical methods are similar to those described for Modena and references therein. Sampling positions for NFHS-2-NP were chosen according to Figure 2 and measured in a random order, resulting in a total number of twenty-one measurements. To account for potential offsets in  $^{87}\text{Sr}/^{86}\text{Sr}$ , JCI-1 was used as the RM



( $^{87}\text{Sr}/^{86}\text{Sr} = 0.70917 \pm 0.00003$ ,  $2s$ ,  $n = 15$ ). Within the same measurement session, JCP-1 was analysed as a QCM ( $^{87}\text{Sr}/^{86}\text{Sr} = 0.70916 \pm 0.00002$ ,  $2s$ ,  $n = 6$ ), as well as two biapatite QCMs to check for matrix-dependent offsets in  $^{87}\text{Sr}/^{86}\text{Sr}$ . A modern shark tooth yielded an  $^{87}\text{Sr}/^{86}\text{Sr}$  of  $0.70919 \pm 0.00002$  ( $2s$ ,  $n = 9$ , Weber *et al.* 2020b) and the African elephant molar AGLOX yielded an  $^{87}\text{Sr}/^{86}\text{Sr}$  ratio of  $0.70992 \pm 0.00012$  ( $2s$ ,  $n = 6$ , Weber *et al.* 2021a). All resulting  $^{87}\text{Sr}/^{86}\text{Sr}$  ratios agree, within uncertainties, with their respective literature value.

### Pb isotope ratios

At GEOMAR (Lab 9A), the Pb chemistry protocol used the same dissolution as for the Sr isotope ratio measurements. Lead separation was carried out using a two pass 150  $\mu\text{l}$  microcolumn procedure filled with BioRad AG<sup>®</sup> 1  $\times$  8 Anion Exchange Resin (Hoernle *et al.* 2008). Lead isotope ratios were determined on a Thermo Scientific<sup>®</sup> TRITON Plus TIMS operating in static multi-collection mode; the mass bias correction undertaken employed the Pb double spike (DS) of Hoernle *et al.* (2011).

The long-term Pb-DS corrected NIST SRM 981 values are  $^{206}\text{Pb}/^{204}\text{Pb} = 16.9408 \pm 0.0018$ ,  $^{207}\text{Pb}/^{204}\text{Pb} = 15.4975 \pm 0.0018$ ,  $^{208}\text{Pb}/^{204}\text{Pb} = 36.7207 \pm 0.0047$ ,  $^{207}\text{Pb}/^{206}\text{Pb} = 0.914804 \pm 0.000049$  and  $^{208}\text{Pb}/^{206}\text{Pb} = 2.167583 \pm 0.000098$  ( $2s$ ,  $n = 169$ ) and lie well within the recommended NIST SRM 981 poly-spike values of Taylor *et al.* (2014). Total chemistry blanks were  $< 30$  pg Pb and thus considered negligible relative to the amounts of sample used. A QCM of leached BCR-2 (USGS) gave  $^{206}\text{Pb}/^{204}\text{Pb} = 18.8033 \pm 0.0005$ ,  $^{207}\text{Pb}/^{204}\text{Pb} = 15.6242 \pm 0.0005$ ,  $^{208}\text{Pb}/^{204}\text{Pb} = 38.8271 \pm 0.00016$  (2SE repeatability for all) and are within those of Fourny *et al.* (2016) and Todd *et al.* (2015) for leached BCR-2.

### $\delta^{13}\text{C}$ and $\delta^{18}\text{O}$ values

$\delta^{13}\text{C}$  and  $\delta^{18}\text{O}$  values were determined by five laboratories, AWI (Lab 1B), GEOMAR (Lab 9B), MARUM (Lab 11), NIOZ (Lab 3C) and UC Davis (Lab 12), using automated carbonate preparation devices the principle of which applies to all instruments, regardless of manufacturer (Fisons Optima IRMS, KIEL IV systems coupled to a MAT252, MAT253(plus)).

In the automated carbonate preparation device, samples and RMs react with phosphoric acid at temperatures of 70–90 °C (Table S1) to form  $\text{CaHPO}_4$  (precipitate),  $\text{H}_2\text{O}$  and  $\text{CO}_2$  (Swart *et al.* 1991). After separating the  $\text{CO}_2$  from water vapour using a cryogenic trap, the  $\text{CO}_2$  is measured

using a sector field gas IRMS. Three laboratories measured NFHS-2-NP against NBS-19, while two laboratories against their respective house RMs, themselves calibrated against NBS-19 (Table S1).

To examine the potential different behaviour of the very fine-grained NFHS-2-NP, NIOZ (Lab 3C) performed an experiment leaving the RM in prolonged contact with humid air (in contrast to storage in a drying cabinet or desiccator). The increased specific surface area of the powder makes it potentially more susceptible to adsorption of moisture from air. Consequently, we cannot exclude *a priori* a slow reaction/recrystallisation in the presence of absorbed water and changing  $\delta^{18}\text{O}$  values by oxygen exchange. NFHS-2-NP was first dried at 105 °C for 3 h, split into six aliquots and transferred to six glass bottles. One bottle was closed immediately and kept in a desiccator. The other five bottles were kept open in a laminar flow hood class 5 (preventing contamination from external sources), and in contact with air with a humidity of 45–57%. Each week a bottle was closed with aluminium caps with rubber seals, sealed with parafilm and stored in a desiccator upon analysis. Each subsequent bottle had 1 week additional and potential reaction time. The sixth and final sample had accordingly been in contact with humid air for 5 weeks. All samples were measured five or six times in a random order in two sequences.

### Data evaluation

To yield reference values for the mass fractions, data obtained by bulk analyses of forty-six elements by laboratories 1–6 were evaluated following ISO (2017) and ISO Guide (2017). A prerequisite for this approach is that the values in the dataset are approximately normally distributed. This was tested here by applying a Kolmogorov-Smirnov test and a Grubbs test to identify outliers. Identified outliers were not removed unless there was a clear, technical/analytical reason that explained the aberrant value(s). Accordingly, the assigned values were calculated by applying Equation (1) (ISO Guide 35:2017 Annex A.2.4. equation A.1). We refer to these assigned values as the *mean of means* throughout this paper.

$$\text{Mean of means} = \frac{\sum y_i}{p} \quad (1)$$

where  $y$  is the arithmetic mean and  $p$  the number of data sets.

Second, the uncertainty component for this value was calculated using Equation (2) (ISO Guide 35:2017 Annex

A2.5.3, equation A4). We refer to this uncertainty component as *reproducibility* throughout the paper.

$$\text{Reproducibility} = \frac{\text{Standard deviation } (y)}{\sqrt{p}} \quad (2)$$

Then, the *expanded reproducibility* was calculated using Equation (3):

$$\text{Expanded reproducibility} = \text{Reproducibility} \times k \quad (3)$$

The expansion factor ( $k$ ) is determined by the effective degrees of freedom within our dataset assuming a normal distribution. The degrees of freedom are obtained by subtracting the number of observations for each dataset. Thus, if two laboratories provide five data points, the number of observations is ten and degrees of freedom = 8. If the effective degrees of freedom are > 10, this factor is  $k = 2$  (ISO Guide 35 2017, 10.4). If the effective degrees of freedom are < 10, the appropriate factor from a Student's  $t$  distribution should be applied. In this case, the reproducibility is represented at the 95% confidence level using a factor of  $k = 2$  because all assigned values have > 10 degrees of freedom. No fully ISO compliant homogeneity or stability test was performed on the pellets. Therefore, the real reproducibility will be higher. However, homogeneity and stability usually contribute the least to the full reproducibility.

We chose to use the Horwitz test (Horwitz and Albert 1995) to evaluate the reproducibility of all mass fractions determined for the forty-six elements by laboratories 1–6. This test calculates an expected relative standard deviation (RSD; Equation 4) based on the analyte's mass fraction  $C$  expressed as a decimal fraction (i.e., 1%  $m/m = 0.01$ ), which is subsequently compared with the measured RSD (Equation 5):

$$\text{RSD}\%_{\text{expected}} = 2 \times C^{(-0.1505)} \quad (4)$$

$$\text{RSD}\%_{\text{measured}} = \frac{\text{Expanded reproducibility}}{\text{Mean of means}} \times 100 \quad (5)$$

$$\text{HORRAT} = \frac{\text{RSD}\%_{\text{measured}}}{\text{RSD}\%_{\text{expected}}} \quad (6)$$

The resulting ratio, called the *Horwitz ratio* (HORRAT, Equation 6), indicates whether precision is acceptable (HORRAT  $\leq 1$ ) or not (HORRAT close to 2). The calculated expanded reproducibility is based on all participants that provided data for a specific analyte, excluding the LA-ICP-MS data.

In summary, we followed recommendations outlined in ISO guides (see reference list). Practically, after applying the Kolmogorov-Smirnov test to check for a normal distribution and a Grubbs test to identify outliers, we calculated the mean of means, the reproducibility and the expanded reproducibility, and finally performed a Horwitz test to compare the measured RSD with the expected RSD. The criteria for classification of the mean of means into reference and information values are (a) data from more than one laboratory, and (b) useable reproducibility using a Horwitz test.

Pellet homogeneity was evaluated according to the ASTM Guide E826-14 (2014). Homogeneity can be evaluated on element to calcium ratios or on element mass fractions. This will result in equal results. Details of data evaluation of pellet homogeneity are given in Appendix A.

## Results and discussion

### Elemental mass fraction – reference and information values

The mass fractions of forty-six elements are listed in Table S2 and those of ten selected elements relevant for palaeoclimate studies and proxy application (i.e., B, Ba, Cd, Li, Mg, Mn, Na, Pb, Sr and Zn) are shown in Figure 3. Element mass fraction values are in overall agreement (a) when comparing results between laboratories and (b) across methods (Figure 3). For the selected elements, the mean of means and expanded reproducibility are shown as a horizontal line and green band respectively (Figure 3). In general, the mean of means and reproducibility were derived from solution techniques. In this case, the Li-borate fusion and XRF analysis are counted among them, as the sample matrix was decomposed. In contrast, the results of LA-ICP-MS (ID. 3B and 7A, Figure 3) were not included in the calculation as all methods should be traceable to the SI-unit and derived following protocols in compliance with ISO (2018). It should be noted that laser ablation data are in close agreement with the mean of means.

A HORRAT test is one way to divide elements into reference or information values. Of all forty-six determined element mass fractions, thirty-six have a HORRAT < 1 (Figure 4) and are therefore sufficiently well-constrained to serve as reference values. Considering the age of the publication (Horwitz and Albert 1995) and the increase in analytical instrument quality and hence data produced since then, we deliberately set the maximum precision limit at HORRAT = 1 (instead of 2). In addition, we here also used the expanded reproducibility (Equation 3) to calculate the

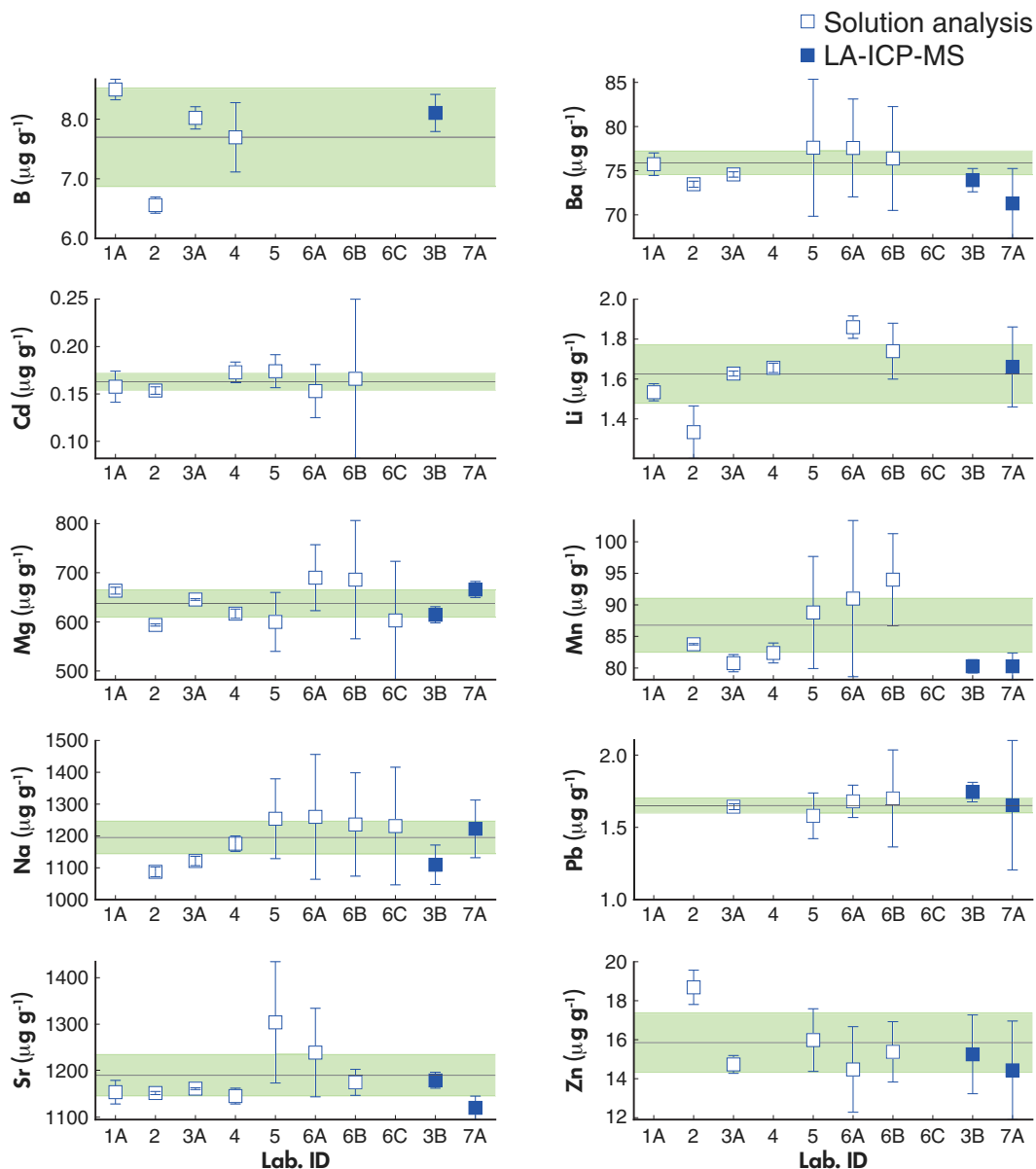


**Figure 3. Element mass fractions of NFHS-2-NP reported by the various participating laboratories (1–7). Laboratories 1–5 used solution ICP-MS, 6A and 6B applied two different total digestion methods and applied ICP-MS, ICP-OES, 6C applied XRF, and 3B and 7A determined the composition of the NFHS-2-NP using LA-ICP-MS. Range bars represent the repeatability precision (95% CL) of the individual laboratories. The horizontal line represents the mean of means. The green band represents the expanded reproducibility (Equation 3).**

RSD. Without the application of this coverage factor ( $k$ ), the reproducibility would be lower by a factor of 2. For the elements, Al, Cr, Fe, Hf, K, P, S, Ti, U, V and Zr HORRAT values  $> 1$  indicate insufficient reproducibility for the mass fractions to be used as reference values (Figure 4) and are therefore stated as information values (Appendix S1).

In addition to those elements that show insufficient reproducibility, the Al and Fe mass fractions of  $641 \pm 45$

and  $532 \pm 36 \mu\text{g g}^{-1}$ , respectively (Appendix S1), are high when compared with the values expected for planktic foraminiferal carbonate (Johnstone *et al.* 2016). Both elements are often used to indicate potential exogenous contamination (e.g., by adhered clay particles or oxide overgrowths). Following observations of insufficient reproducibility of several elements and an offset of Al and Fe between laboratories using  $\text{HNO}_3$  dissolution and total digestion, NIOZ directly compared twenty-three elements

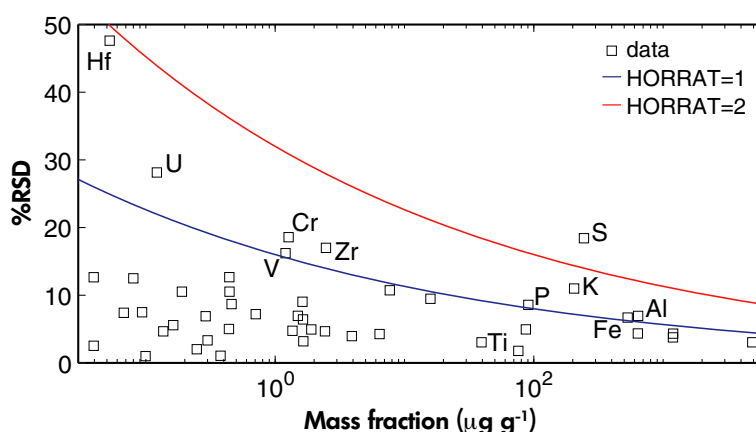


**Figure 4.** Measured RSD against mass fraction (log scale). Several elements with HORRAT above 1 (blue curve, the upper red curve indicated HORRAT = 2) indicate insufficient reproducibility based on the Horwitz classification. The thirty-six elements with an approved reproducibility (below the blue curve) are not labelled.

from NFHS-2-NP using two dissolution methods. We found that the values were similar for B, Ba, Mg, Mn, Na, P, Pb, Sr and Zn using both methods (Table S3). However, the total digestion values were higher for Cu, Li and U, being considerably higher for S, Rb, Fe, K, V, Al and Cr (10, 14, 17, 21, 26, 30 and 32% respectively) than using HNO<sub>3</sub> only (Table S3). These elements also showed the poorest reproducibility when comparing results from the different

participants using different dissolution methods (total digestion, Li-borate fusion, HNO<sub>3</sub> only; Figure 4).

HNO<sub>3</sub> dissolution, in this case, is believed to only extract the HNO<sub>3</sub>-soluble fraction from the milled powder. Milling is always an abrasive process and since the foraminifera were milled in both zirconium oxide and agate (SiO<sub>2</sub>) beakers, a contamination of the resulting powder of NFHS-2-NP with SiO<sub>2</sub> and ZrO<sub>2</sub> and lattice-bound elements in both materials is likely. Since neither of these is soluble in HNO<sub>3</sub>, it is very likely that mass fractions will be underestimated if only HNO<sub>3</sub> is used for dissolution. Based on these observations, we hypothesise the presence of a refractory fraction in the powder. Aluminium and Fe could originate from aluminium and iron silicates from the zirconia milling gear; however currently, there is no available information that this milling gear contains S, Rb, K, V and Cr. The refractory fraction may also originate from clays. The relatively low boron and magnesium mass fractions, however, contradict this hypothesis. In conclusion, there is a refractory fraction or phase of yet unclear origin in the powder, which can only be fully accounted for when using a more severe dissolution method than nitric acid. The generally good correlation between LA-ICP-MS and total digestion for these refractory elements (e.g., Al, see Figure 5) confirms this.

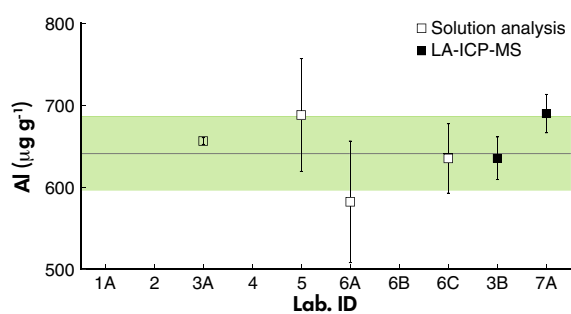


**Figure 5.** Mass fraction of Al reported by the various participating laboratories (1–7). Labs 3A and 5 used ICP-MS after total digestion, 6A, 6B applied two different total digestion methods and 6C applied XRF, 3B and 7A determined the composition of the NFHS-2-NP using LA-ICP-MS (Labs 1A, 2 and 4 used ICP-MS after digestion with nitric acid only and data are removed). Range bars represent the repeatability (95% CL) of the individual laboratories. The green band represents the expanded reproducibility (Equation 3) of the mean of means derived from total digestion and XRF techniques.

Total digestion using HF in combination with other strong acids is more comparable to laser ablation, which can be considered a bulk analytical technique where all the material ablated is analysed by ICP-MS. As a result of the observation of all laboratories and the NIOZ comparison, the data of Al, Fe and V from the laboratories using only HNO<sub>3</sub> to dissolve the nano-milled carbonate

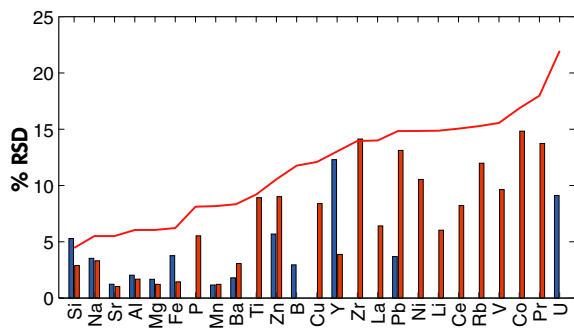


**Figure 6.** %RSD of elements measured by NIOZ (lab 3B, in blue) and JGU (lab 7A, in red) using LA-ICP-MS using 60 and 70  $\mu\text{m}$  spot sizes respectively. The red line represents the expected (maximum) RSD calculated using the Horwitz equation (Equation 4).

powder of NFHS-2-NP were not included in the calculation. The data of S, Rb, K and Cr, with lower reproducibility, were all included as they were obtained from participants using total digestion. Of the elements relevant for environmental research B, Ba, Cd, Li, Mg, Mn, Na, Sr and Zn will be published as reference values whereas U with a low reproducibility will be published as an information value.

### Elemental mass fraction – homogeneity

An ASTM Guide 826 E14 test was applied on all the LA-ICP-MS mass fraction data to check for inter- and intra-pellet homogeneity. All elements passed this test and the pellets showed homogeneity for all forty-six monitored elements when analysed using a spot size of 60–70  $\mu\text{m}$ .

The level of homogeneity per element can be expressed as the RSD for the measured concentration within a pellet. All measured elements are shown in Figure 6 and Table S4. The RSD of elements relevant as proxies for palaeoclimate research (i.e., B, Ba, Li, Mg, Mn, Na, Sr and Zn) are < 3% and similar to the variability of those elements in the NIST SRM 61x glasses (Jochum *et al.* 2011). Elements P, Ti, V and Zr are those with poor reproducibility but are considered as less important elements for palaeoclimate research.

Figure 7 shows a comparison of the repeatability (RSD %) as an indicator for homogeneity of three NPs (JCp-1 NP, JCl-1 NP and MACS-3 NP) and the original USGS MACS-3 (data from Jochum *et al.* 2019) analysed with a spot size of 55  $\mu\text{m}$ , and the repeatability (RSD%) of NFHS-2-NP of this study determined by NIOZ and JGU. The lower RSDs of

MACS-3 NP compared with USGS MACS-3 shows the improved homogeneity because of the nano-milling process. Homogeneity of NFHS-2-NP measured with a spot size of 60 and 70  $\mu\text{m}$  is similar to that of JCp-1 NP and JCl-1 NP measured with a spot size of 55  $\mu\text{m}$ . MACS-3 NP seems to be more homogeneous than JCp-1 NP and JCl-1 NP. Looking at a threshold of < 3% RSD, we can conclude that most data corresponding with MACS-3 NP and NFHS-2-NP fall in this range. These data of NFHS-2-NP in the range < 3% are the elements relevant for palaeoclimate research. Some RSDs in NFHS-2-NP of in general elements with mass fractions < 10  $\mu\text{g g}^{-1}$  are relatively high in comparison with the other RMs and are thus less well distributed in the pellet. These elements include P, Ti, V and Zr with poor reproducibility (Figure 6).

Most elements and especially elements relevant as proxies for palaeoclimate research are distributed homogeneously when considering the data obtained by LA-ICP-MS in this study, implying that the pellet is suitable for *in situ* techniques targeting these elements using spot sizes of approximately 60  $\mu\text{m}$  and above. Also, when refractory elements (e.g., Al and Fe) are used to indicate detrital contamination in foraminifera shells, this pellet may serve as a QCM.

### $^{87}\text{Sr}/^{86}\text{Sr}$ – reference values and homogeneity

A compilation of all Sr isotope data is provided in Table S5. Figure 8 shows the results of  $^{87}\text{Sr}/^{86}\text{Sr}$  isotope ratio measurements of NFHS-2-NP.  $^{87}\text{Sr}/^{86}\text{Sr}$  isotope ratios of the powder were determined by three different laboratories using TIMS and solution MC-ICP-MS (ID 1–3, Figure 8) and yielded a mean of means and expanded reproducibility of  $^{87}\text{Sr}/^{86}\text{Sr}$  of  $0.709163 \pm 0.000008$ , which is in good agreement with  $^{87}\text{Sr}/^{86}\text{Sr}$  of 0.70917 Pleistocene seawater values (McArthur *et al.* 2012). The foraminifera were collected from a section of a piston core with an estimated age of 450–540 ka based on six  $^{14}\text{C}$  measurements from a box core taken at the same location, assuming that the sedimentation rate was constant (Lončarić *et al.* 2007). In addition to the mean  $^{87}\text{Sr}/^{86}\text{Sr}$  isotope ratios, we report individually measured  $^{87}\text{Sr}/^{86}\text{Sr}$  isotope ratios for all participants (Table S6). Replicate analysis of NFHS-2-NP of GEOMAR (Lab 9A) by means of a second digest were within 2s of NIST SRM 987 mentioned and indicate homogeneity of NFHS-2-NP at a test portion size of 100 mg (Figure 8; Table S6).

In addition, JGU and Modena used LA-MC-ICP-MS to evaluate the homogeneity of NFHS-2-NP for  $^{87}\text{Sr}/^{86}\text{Sr}$ . The LA-MC-ICP-MS analyses (Figure 8) yielded mean  $^{87}\text{Sr}/^{86}\text{Sr}$  ratios and repeatability of  $0.70918 \pm 0.00005$  (2s,



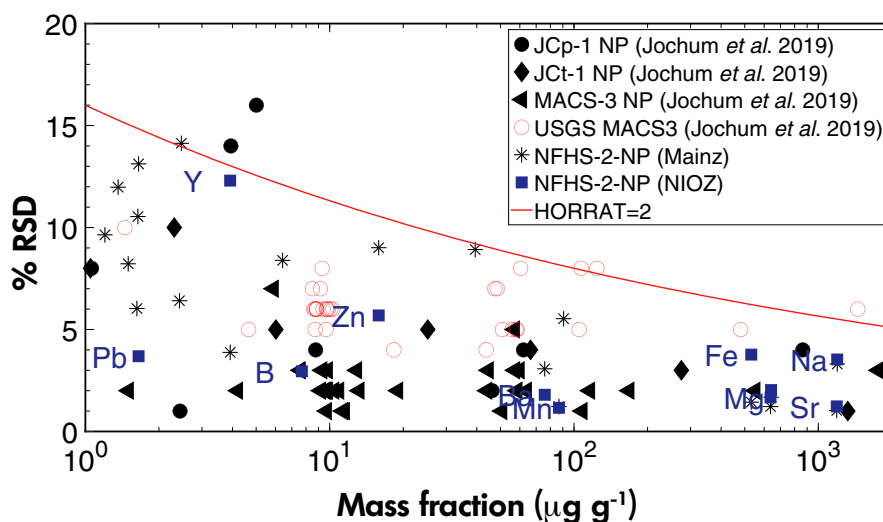


**Figure 7.** RSD of JcP-1 NP, JcT-1 NP, MACS-3 NP, USGS MACS-3 and NFHS-2-NP against elemental mass fraction in  $\mu\text{g g}^{-1}$  (log-scale). For the simplicity of the plot, only the NIOZ values are labelled and trace elements with extreme low mass fractions  $< 1 \mu\text{g g}^{-1}$  are not shown. Elements relevant for environmental research measured by NIOZ and Mainz were in close agreement (Figure 6).

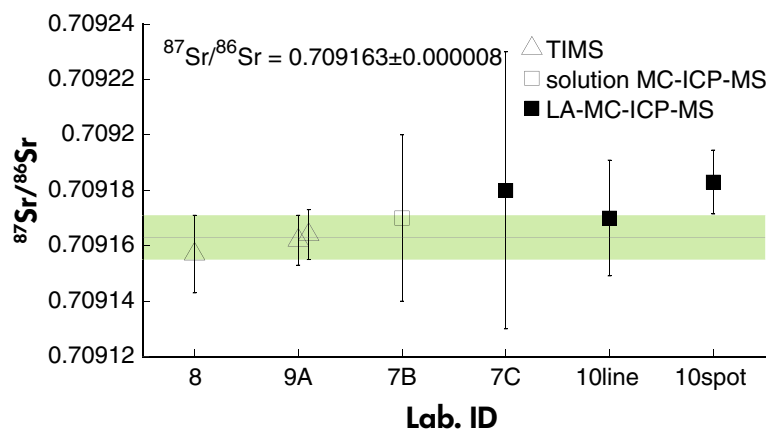


**Figure 8.**  $^{87}\text{Sr}/^{86}\text{Sr}$  ratio against laboratory ID. The horizontal line represents the mean of means derived from TIMS and solution MC-ICP-MS. The green band represents the expanded reproducibility (Equation 3) of the mean of means. Range bars represent the 2s repeatability precision of the individual laboratories.

$n = 21$ , Lab 7C, line scan with a line length of  $500 \mu\text{m}$  and spot size of  $70 \mu\text{m}$ ,  $0.70917 \pm 0.00002$  ( $2s$ ,  $n = 12$ , Lab 10line, line scan with a length of  $600 \mu\text{m}$  and spot size of  $100 \mu\text{m}$ ) and  $0.70918 \pm 0.00001$  ( $2s$ ,  $n = 3$ , Lab 10spot, spot analysis with a spot size of  $80 \mu\text{m}$ ) respectively. These mean LA-MC-ICP-MS values agree well with TIMS and solution MC-ICP-MS analyses. The repeatability ( $2s$ ) of  $0.00005$ ,  $0.00002$  and  $0.00001$  is good and shows homogeneity for the Sr isotope ratios at the spot sizes used.

### Pb isotope ratios – information values

The results of the Pb isotope ratios measured at GEOMAR can be found in Table 4. Replicate analysis of NFHS-2-NP by means of a second digest is within  $2s$  of NIST SRM 981 and proves high precision and indicates homogeneity of NFHS-2-NP at a test portion size of  $100 \text{mg}$ . These data are useful to perform matrix-matched external mass bias correction during LA-(MC)-ICP-MS for Pb isotope ratios using these values from bulk analysis of NFHS-2-NP.

## $\delta^{13}\text{C}$ and $\delta^{18}\text{O}$ – information values

The  $\delta^{13}\text{C}$  and  $\delta^{18}\text{O}$  values were determined by five laboratories and are shown in Table S1. The number of individual analyses per laboratory was in the range 5–90. Figure 9 shows for each laboratory the results of the mean and repeatability precision (1 $\sigma$ ). The mean of means of all laboratories with an expanded reproducibility (95% CL) of  $\delta^{13}\text{C}_{\text{VPDB}}$  and  $\delta^{18}\text{O}_{\text{VPDB}}$  is  $0.79 \pm 0.04$  and  $-0.04 \pm 0.05\text{‰}$  respectively. The significantly lower  $\delta^{18}\text{O}$  values (second table of S1) of NFHS-2-NP stored at the institutes for longer than 1 year (discussed below) were excluded from the mean of means.

After more than 1 year of storage in a desiccator or sealed bag, analyses of NFHS-2-NP were repeated by NIOZ, AWI and MARUM using the original sample aliquots and storage bottles. This showed that the original  $\delta^{18}\text{O}$  value of  $-0.04 \pm 0.05\text{‰}$  drifted to  $-0.25$ ,  $-0.39$  and  $-0.44\text{‰}$  measured by NIOZ, MARUM and AWI respectively (second Table S1, data are not included in Figure 9). The QCMs measured by these three laboratories showed high accuracies (Table S1) for all measurements excluding that this offset was caused by instrumental issues. Moreover, measurement by MARUM of a second batch, stored at myStandards GmbH for 2 years, reproduced the original data of MARUM from the first batch (Table S1, batch 2, not included in the mean of means), confirming the long-term  $\delta^{18}\text{O}$  drift of the first batch stored at MARUM. A cross calibration between MARUM and NIOZ by exchanging vials confirmed that (a) the  $\delta^{18}\text{O}$  value of MARUM's batch drifted to lower values ( $-0.39 \pm 0.05\text{‰}$  ( $n = 8$ ) measured by MARUM and  $-0.50 \pm 0.07$  ( $n = 6$ ) measured by NIOZ), and (b) that the  $\delta^{18}\text{O}$  value of NIOZ's batch also drifted to lower values ( $-0.24 \pm 0.13\text{‰}$  ( $n = 2$ ) measured by MARUM and  $-0.25 \pm 0.07$  ( $n = 6$ ) measured by NIOZ).

A reason for the observed offset could be contact with humid air during the weighing step in the laboratory in combination with the high specific surface area of NFHS-2-NP. NIOZ tested the effect of exposing NFHS-2-NP to moisture for durations of 0 ( $t = 0$ ) to 36 days ( $t = 36$ , ~ 5 weeks). Results show that such exposure did not alter the  $\delta^{13}\text{C}$  or  $\delta^{18}\text{O}$  values at NIOZ (Figure 10). Over the duration of the experiment, the values of the dry powder ( $t = 0$ ) of both stable isotopes remained constant, within the repeatability precision of the measurement. This does not exclude resetting of isotopes when stored over longer time periods in the presence of moisture, and hence, we still recommend storing the material in a desiccator, as is common practice for RMs. However, we concluded from this experiment that contact with humid air, during a time span of 5 weeks, was not the reason for the observed offset.

NFHS-2NP was made by nano-milling NFHS-1. NFHS1 is coarser grained and used at NIOZ as an in-house RM for stable isotope measurements. Information values of the mean of means of this RM analysed at Cardiff University, the University of Utrecht, UU and NIOZ for  $\delta^{13}\text{C}_{\text{VPDB}}$  and  $\delta^{18}\text{O}_{\text{VPDB}}$  are  $0.84 \pm 0.02$  and  $1.11 \pm 0.06\text{‰}$ . The  $\delta^{18}\text{O}$  values in NFHS1 are stable since 2014. Interestingly, the  $\delta^{18}\text{O}$  of NFHS-2-NP (thus *after* nano-milling) is  $-0.04 \pm 0.05\text{‰}$  and significantly lower than  $\delta^{18}\text{O}$  of NFHS1 of  $1.11 \pm 0.06\text{‰}$  (*before* milling). Mass fractions of NFHS1 (not shown) were measured at NIOZ and showed an almost identical composition as NFHS-2-NP; however, NFHS-2-NP is finer grained and contains more  $\text{SiO}_2$  than NFHS1. This  $\text{SiO}_2$  cannot cause a change in the  $\delta^{18}\text{O}$  values because no  $\text{CO}_2$  is produced by dissolution with phosphoric acid in the automated carbonate preparation device. Therefore, we have no explanation for the observed difference between the  $\delta^{18}\text{O}$  values of NFHS1 and NFHS-2-NP. Research is needed to investigate how the nano-milling procedure

**Table 4.** Results of Pb isotope ratio measurements of NFHS-2 NP by TIMS (Thermo Scientific® TRITON Plus) at GEOMAR (Lab 9A) along with RM USGS BCR-2

Ratio	NFHS-2-NP digest A		NFHS-2-NP digest B		BCR-2	
	Unleached		Unleached		2 mol l <sup>-1</sup> HCl @ 70 °C for 1 h	
	Mean	2SE	Mean	2SE	Mean	2SE
<sup>206</sup> Pb/ <sup>204</sup> Pb	17.8572	0.0007	17.8584	0.0009	18.8033	0.0005
<sup>207</sup> Pb/ <sup>204</sup> Pb	15.5907	0.0006	15.5911	0.0007	15.6242	0.0005
<sup>208</sup> Pb/ <sup>204</sup> Pb	37.7701	0.0016	37.7706	0.0019	38.8271	0.0016
<sup>207</sup> Pb/ <sup>206</sup> Pb	0.873075	0.000009	0.873040	0.000011	0.830931	0.000008
<sup>208</sup> Pb/ <sup>206</sup> Pb	2.115121	0.000021	2.115008	0.000021	2.064913	0.000043

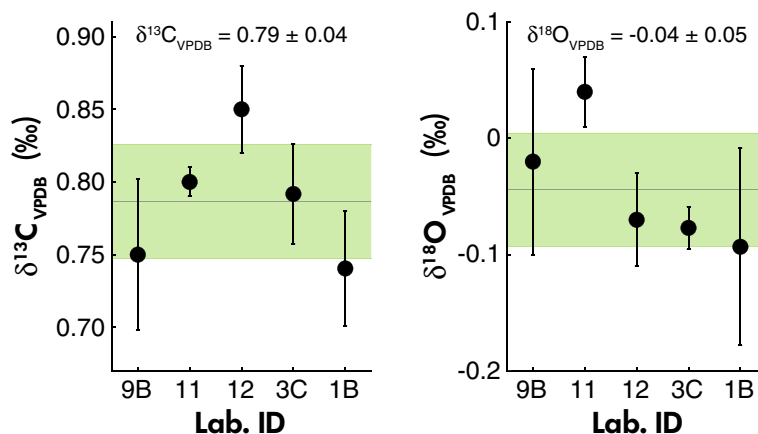


**Figure 9.**  $\delta^{13}\text{C}$  and  $\delta^{18}\text{O}$  values obtained for NFHS-2-NP against laboratory ID. The horizontal line represents the mean of means derived from five participants. The green band represents the expanded reproducibility (Equation 3). The individual range bars reflect the repeatability (1 s) of each laboratory.

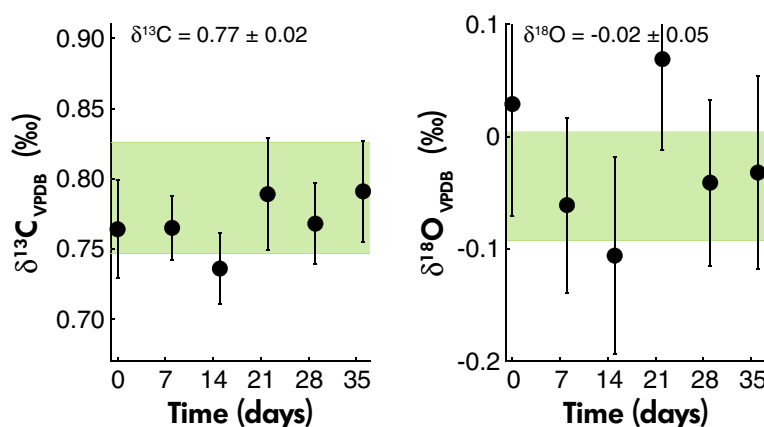


**Figure 10.**  $\delta^{13}\text{C}$  and  $\delta^{18}\text{O}$  against time in days to test for potential impact of moisture absorption. NFHS-2-NP was analysed five or six times per batch by NIOZ. The green band represents the expanded reproducibility (Equation 3) derived from the five participants.

changed the  $\delta^{18}\text{O}$  value. Research is needed to check whether and how time changed the  $\delta^{18}\text{O}$  value at AWI, MARUM and NIOZ while the  $\delta^{18}\text{O}$  value of NFHS-2-NP stored at myStandards GmbH remained stable.

The pellets of NFHS-2-NP with information values for  $\delta^{13}\text{C}_{\text{VPDB}}$  and  $\delta^{18}\text{O}_{\text{VPDB}}$  of  $0.79 \pm 0.04$  and  $-0.04 \pm 0.05\text{‰}$ , respectively, are intended to be used for SIMS analyses. However, more testing regarding pellet stability under high-vacuum conditions and ion beam is required before we are confident to distribute it for this purpose. Thus, stable isotopes by SIMS measurements remain to be tested. For the SIMS application, we hope that our  $\delta^{13}\text{C}$  and  $\delta^{18}\text{O}$  information values combined with *in situ* mass fraction and Sr isotope ratios will be useful.

### NFHS-2-NP as a matrix-matched calibration RM

At NIOZ, NFHS-2-NP was first measured as an unknown material with LA-ICP-MS, together with four different NP QCMs and USGS MACS-3, using NIST SRM 610 as a calibration RM. After reference values of the new RM were established in the context of this study, NFHS-2-NP was used as a calibration RM to obtain data for the QCMs JcP-1 NP, JcT-1 NP and ECRM752 NP, which are close in composition to NFHS-2-NP to test its applicability as calibration material when analysing carbonate samples. It should be noted that the mass fraction of Sr in JcP-1 NP is higher than in NFHS-2-NP and NIST SRM 610; thus, Sr data can only be obtained by extrapolation, which can lead to inaccuracies. The Sr mass fraction of JcP-1 NP is more similar to USGS MACS-3 or

MACS-3 NP. For Sr mass fractions in aragonite marine carbonates, USGS MACS-3 or MACS-3 NP could be a better calibration RM. Table 5 shows the mass fraction of those elements measured at NIOZ and where reference values of NFHS-2-NP are known. It shows that data of all elements using NFHS-2-NP as a calibration RM agree, within repeatability precision, with data using NIST SRM 610 as a calibration RM. NFHS-2-NP could therefore be an alternative for or in combination with, for example NIST SRM 610 and/or NIST SRM 612 to calibrate LA-ICP-MS measurements on carbonate samples. For some matrix sensitive elements (e.g., Na, Pb and Zn) in natural calcite samples, it could be a better alternative than silicate glass RMs.

Compared with non-NP RMs such as USGS MACS-3, NFHS-2-NP could be a better alternative for the analysis of natural calcite samples for two reasons: (a) because of the discussed improved homogeneity, and (b) because the improved cohesion of NPs is beneficial for laser ablation analysis, as already pointed out by Garbe-Schönberg and Müller (2014), who highlighted the smooth surfaces of the tablet, and that the crater walls and bottom are similar to ablation pits in glass. Therefore, for determination of mass fractions, the ablation behaviour should be quite similar to a solid sample including carbonates. The calcite RM NFHS-2-NP could therefore have similar ablation rates and crater aspect ratio as natural crystalline calcite material (e.g., foraminifera). If there is still a difference in ablation rate between a natural sample and RM, the internal standard Ca could correct for bias.

However, for isotopic determinations, Guillong *et al.* (2020) suggested that carbonate U-Pb dating by LA-ICP-MS is only accurate when the laser ablation crater aspect ratio is similar for the RM and unknown sample. The authors concluded that the ablation rates in natural samples of dolomite and aragonite are 1.6 and 2 times larger than in

calcite, causing different crater aspect ratios. In this study, U-Pb were not measured; however,  $^{87}\text{Sr}/^{86}\text{Sr}$  was studied in detail. Table 6 highlights the QCMs described in the LA-MC-ICP-MS method section of Modena and JGU.

All resulting  $^{87}\text{Sr}/^{86}\text{Sr}$  ratios agree, within repeatability precision, with their respective literature value derived from solution MC-ICP-MS/TIMS or modern seawater values. The high accuracies of the QCM measurements as shown in Table 6 together with our NFHS-2-NP results (Figure 8, Table S5) where LA-MC-ICP-MS values agree with TIMS and solution MC-ICP-MS analyses, leads us to the conclusion that for this kind of carbonate samples matrix matching using crystalline RMs is not crucial for *in situ* Sr isotope measurements.

While the use of nano-pellets in LA-ICP-MS has been increasing in the recent years, it remains to be shown that the matrix matching is true and how ablation behaviour affects other isotope systems and determined ratios (e.g.,  $\delta^{11}\text{B}$ ). The isotopes  $^{10}\text{B}$  and  $^{11}\text{B}$  have a relatively larger mass difference than  $^{87}\text{Sr}$  and  $^{86}\text{Sr}$ .  $\delta^{11}\text{B}$  could therefore, or for other unknown reasons, be more sensitive to fractionation. NFHS-2-NP could therefore become an important matrix-matched calibration RM for  $\delta^{11}\text{B}$  measurement in natural calcite samples using *in situ* techniques.

## Conclusions

We present a new carbonate RM NFHS-2-NP, made from shells of fossil planktic foraminifera that were ground using a nano-milling technique and pressed into pellets without any binder. Twelve independent laboratories analysed this new RM (powder and pellets) applying various techniques. The obtained elemental and isotopic data confirm the homogeneity of NFHS-2-NP and therefore its usability for calibration or monitoring the quality of *in situ* measurements by techniques such as LA-(MC)-ICP-MS and  $\mu\text{XRF}$ .

**Table 5.** Element mass fractions ( $\mu\text{g g}^{-1}$ ) determined by LA-ICP-MS at NIOZ with 60  $\mu\text{m}$  circular spots on different carbonate QCMs applying NFHS-2-NP and NIST SRM 610 as calibration materials (CAL RM)

QCM:	JCp-1 NP				JCr-1 NP				ECRM752 NP			
	NFHS-2-NP		NIST SRM 610		NFHS-2-NP		NIST SRM 610		NFHS-2-NP		NIST SRM 610	
	Mean	1 s	Mean	1 s	Mean	1 s	Mean	1 s	Mean	1 s	Mean	1 s
B	42	4	45	5	18	3	19	3	2.1	0.1	2.3	0.1
Ba	12	2	12	1	10	3	10	3	62	5	60	5
Mg	858	93	849	92	271	13	268	13	890	11	882	11
Mn	1.09	0.06	1.01	0.06	0.48	0.07	0.45	0.07	83	2	77	1
Na	4146	469	4184	473	3872	186	3908	188	49	5	49	5
Pb	0.25	0.02	0.25	0.02	0.14	0.02	0.14	0.02	1.5	0.1	1.5	0.1
Sr	7477	76	7418	76	1454	20	1443	20	160	1	159	1
Zn	0.9	0.1	0.9	0.1	0.79	0.08	0.76	0.07	4.9	0.6	4.8	0.6

**Table 6.**  
Measured  $^{87}\text{Sr}/^{86}\text{Sr}$  ratios during this study together with reference values

Lab ID	RM	Measured $^{87}\text{Sr}/^{86}\text{Sr}$			Reference $^{87}\text{Sr}/^{86}\text{Sr}$		
		Mean	1 s	n	Mean	1 s	Comment
JGU (Lab 7)	JCt-1	0.70917	0.00003	15	0.70916	0.00006	Weber <i>et al.</i> (2018, GGR)
	JCp-1	0.70916	0.00002	6	0.709164		Weber <i>et al.</i> (2018, GGR)
	AGLOX	0.70992	0.00012	6	0.70999		In-house RM, African elephant molar, Weber <i>et al.</i> (2021a)
	Shark	0.70919	0.00002	9	0.70918		Modern seawater value (shark teeth)
Modena (Lab 10)	Modern seashell	0.70918	0.00002	5	0.70917	0.00003	Modern seawater value
	NanoSr	0.70753	0.00001	2	0.70756		Weber <i>et al.</i> (2020a, GGR)

We provide reference and information mass fraction values for forty-six elements in a product information sheet (Appendix S1). For  $^{87}\text{Sr}/^{86}\text{Sr}$ , we determined a reference value with expanded reproducibility of  $0.709163 \pm 0.000008$ . Information values for  $\delta^{13}\text{C}_{\text{VPDB}}$  and  $\delta^{18}\text{O}_{\text{VPDB}}$  are  $0.79 \pm 0.04$  and  $-0.04 \pm 0.05\text{‰}$  (95% CL) respectively. Regarding Pb isotope ratios, we established information values, that is  $^{206}\text{Pb}/^{204}\text{Pb} = 17.858$ ,  $^{207}\text{Pb}/^{204}\text{Pb} = 15.591$ ,  $^{208}\text{Pb}/^{204}\text{Pb} = 37.770$ ,  $^{207}\text{Pb}/^{206}\text{Pb} = 0.87306$  and  $^{208}\text{Pb}/^{206}\text{Pb} = 2.11506$ .

To use NFHS-2-NP as a RM for microanalytical techniques, homogeneity at micrometre-scale is essential. LA-ICP-MS results confirm that the RSD of several elements relevant for climate research (e.g., B, Na, Mg, Mn, Zn, Sr, Ba and Pb) is < 3% at spot sizes of 60 and 70  $\mu\text{m}$ , indicating a high degree of homogeneity similar to NIST SRM 61x glasses and JCp-1 NP and JCt-1 NP measured at a spot size of 55  $\mu\text{m}$  (Jochum *et al.* 2019). The LA-ICP-MS values agree, within reproducibility, with the solution-based reference values for the monitored elements.

In addition to the element mass fractions,  $^{87}\text{Sr}/^{86}\text{Sr}$  ratios determined by LA-MC-ICP-MS agree with solution-based MC-ICP-MS and TIMS analyses and display good repeatabilities of 0.00005 (2s,  $n = 21$ , 70  $\mu\text{m}$  spot size) and 0.00002 (2s,  $n = 12$ , 100  $\mu\text{m}$  spot size), showing that microhomogeneity of the nano-pellet is indeed ensured for this RM.

## Acknowledgements

We thank the cruise leader Professor G.J. Brummer (NIOZ) for providing piston core PE174-15PC from Walvis Ridge. Dr. Inge van Dijk (NIOZ) is thanked for help during the sieving and cleaning of the foraminifera and Patrick Laan (NIOZ) for the help with the SF-ICP-MS analysis at the NIOZ. Pellets are available on request from myStandards GmbH (info@my-standards.com).

## Data availability statement

Measurements results are available in the supporting information data files that accompany this paper.

## References

### Aizawa S. (2008)

Determination of trace elements in carbonate reference samples by instrumental neutron activation analysis. *Journal of Radioanalytical and Nuclear Chemistry*, 278, 349–352.

### Al-Ammar A., Gupta R. and Barnes R. (2000)

Elimination of boron memory effect in inductively coupled plasma-mass spectrometry by ammonia gas injection into spray chamber during analysis. *Spectrochimica Acta Part B*, 55, 629–635.

### Arslan Z. and Paulson A.J. (2002)

Analysis of biogenic carbonates by inductively coupled plasma-mass spectrometry (ICP-MS). Flow injection on-line solid-phase preconcentration for trace element determination in fish otoliths. *Analytical and Bioanalytical Chemistry*, 372, 776–785.

### ASTM Guide E826-14 (2014)

Standard practice for testing homogeneity of a metal lot or batch in solid form by spark atomic emission spectrometry. ASTM International (West Conshohocken, PA). [www.astm.org](http://www.astm.org)

### Barker S., Greaves M. and Elderfield H. (2003)

A study of cleaning procedures used for foraminiferal Mg/Ca paleothermometry. *Geochemistry Geophysics Geosystems*, 4, 1–20.

### Berglund M. and Wieser M.E. (2011)

Isotopic compositions of the elements 2009 (IUPAC Technical Report). *Pure and Applied Chemistry*, 83, 397–410.

### Bougeois L., De Rafelis M., Reichart G.-J., De Nooijer L.J., Nicollin F. and Dupont-Nivet G. (2014)

A high resolution study of trace elements and stable isotopes in oyster shells to estimate central Asian Middle Eocene seasonality. *Chemical Geology*, 363, 200–212.

### Bums S.J., Matter A., Frank N. and Mangini A. (1998)

Speleothem-based paleoclimate record from northern Oman. *Geology*, 26, 499–502.



## references

**De Villiers S., Greaves M. and Elderfield H. (2002)**

An intensity ratio calibration method for the accurate determination of Mg/Ca and Sr/Ca of marine carbonates by ICP-AES. *Geochemistry Geophysics, Geosystems*, 3, 2001GC000169.

**Durand A., Chase Z., Townsend A.T., Noble T., Panietz E. and Goemann K. (2016)**

Improved methodology for the microwave digestion of carbonate-rich environmental samples. *International Journal of Environmental Analytical Chemistry*, 96, 119–136.

**Eggs S.M., Kinsley L.K. and Shelley J.M.G. (1998)**

Deposition and element fractionation processes occurring during atmospheric pressure laser sampling for analysis by ICP-MS. *Applied Surface Science*, 127–129, 278–286.

**Fourny A., Weis D. and Scoates J.S. (2016)**

Comprehensive Pb-Sr-Nd-Hf isotopic, trace element, and mineralogical characterization of mafic to ultramafic rock reference materials. *Geochemistry Geophysics Geosystems*, 17, 739–773.

**Garbe-Schönberg D. and Müller S. (2014)**

Nano-particulate pressed powder tablets for LA-ICP-MS. *Journal of Analytical Atomic Spectrometry*, 29, 990–1000.

**Greaves M., Barker S., Daunt C. and Elderfield H. (2005)**

Accuracy, standardization, and interlaboratory calibration standards for foraminiferal Mg/Ca thermometry. *Geochemistry, Geophysics, Geosystems*, 6, 2004GC000790.

**Guillong M., Meier D.L., Allan M.M., Heinrich C.A. and Yardley B.W. (2008)**

SILLS: A MATLAB-based program for the reduction of laser ablation ICP-MS data of homogeneous materials and inclusions. In: Sylvester P.J. (ed.), *Laser ablation ICP-MS in the Earth sciences: Current practices and outstanding issues*. Mineralogical Association of Canada Short Course Series, 40, 328–333.

**Guillong M., Wotzlaw J.-F., Looser N. and Laurent O. (2020)**

Evaluating the reliability of U-Pb laser ablation inductively coupled plasma-mass spectrometry (LA-ICP-MS) carbonate geochronology: Matrix issues and a potential calcite validation reference material. *Geochronology*, 2, 155–167.

**Hathome E.C., Felis T., James R.H. and Thomas A. (2011)**

Laser ablation ICP-MS screening of corals for diagenetically affected areas applied to Tahiti corals from the last deglaciation. *Geochimica et Cosmochimica Acta*, 75, 1490–1506.

**Hathome E.D., Brian H., Torben S., Patricia G., Moritz Z. and Martin F. (2012)**

Online preconcentration ICP-MS analysis of rare earth elements in seawater. *Geochemistry Geophysics Geosystems*, 13, 1–12.

Hathome E.C., Gagnon A., Felis T., Adkins J., Asami R., Boer W., Caillon N., Case D., Cobb K.M., Douville E., deMenocal P., Eisenhauer A., Garbe-Schönberg D., Geibert W., Goldstein S., Hughen K., Inoue M.,

Kawahata H., Kölling M., Comec F.L., Linsley B.K., McGregor H.V., Montagna P., Nurhati I.S., Quinn T.M., Raddatz J., Rebaubier H., Robinson L., Sadekov A., Sherrell R., Sinclair D., Tudhope A.W., Wei G., Wong H., Wu H.C. and You C.-F. (2013)

Interlaboratory study for coral Sr/Ca and other element/Ca ratio measurements. *Geochemistry Geophysics Geosystems*, 14, 3730–3750.

**Henehan M.J., Foster G.L., Rae J.W.B., Prentice K.C., Erez J., Bostock H.C., Marshall B.J. and Wilson P.A. (2015)**

Evaluating the utility of B/Ca ratios in planktic foraminifera as a proxy for the carbonate system: A case study of *Globigerinoides ruber*. *Geochemistry Geophysics Geosystems*, 16, 1052–1069.

**Hoernle K., Abt D.L., Fischer K.M., Nichols H., Hauff F., Abers G.A., van den Bogaard P., Heydolph K., Alvarado G., Protti M. and Strauch W. (2008)**

Arc-parallel flow in the mantle wedge beneath Costa Rica and Nicaragua. *Nature*, 451, 1094–1097.

**Hoernle K., Hauff F., Kokfelt T.F., Haase K., Garbe-Schönberg C.-D. and Werner R. (2011)**

On- and off-axis chemical heterogeneities along the South Atlantic Mid-Ocean Ridge (5–11°S): Shallow or deep recycling of ocean crust and/or intraplate volcanism? *Earth and Planetary Science Letters*, 306, 86–97.

**Hoogakker B.A.A., Klinkhammer G.P., Elderfield H., Rohling E.J. and Hayward C. (2009)**

Mg/Ca paleothermometry in high salinity environments. *Earth and Planetary Science Letters*, 284, 583–589.

**Horwitz W. and Albert R. (1995)**

Precision in analytical measurements: Expected values and consequences in geochemical analyses. *Fresenius' Journal of Analytical Chemistry*, 351, 507–513.

**Inoue M., Nohara M., Okai T., Suzuki A. and Kawahata H. (2004)**

Concentrations of trace elements in carbonate reference materials Coral JCP-1 and Giant Clam JCT-1 by inductively coupled plasma-mass spectrometry. *Geostandards and Geoanalytical Research*, 28, 411–416.

**Inoue M., Nohara M., Okai T., Suzuki A. and Kawahata H. (2007)**

Concentrations of trace elements in carbonate reference materials coral JCP-1 and giant clam JCT-1 by inductively coupled plasma-mass spectrometry. *Geostandards and Geoanalytical Research*, 28, 411–416.

**ISO 17025 (2018)**

General requirements for the competence of testing and calibration laboratories. *International Organization for Standardization (Geneva)*, 59pp.

**ISO 17034 (2017)**

General requirements for the competence of reference material producers. *International Organization for Standardization (Geneva)*, 65pp.



## references

**ISO Guide 35 (2017)**

Reference materials – Guidance for characterization and assessment of homogeneity and stability. International Organization for Standardization (Geneva), 105pp.

**Jochum K.P., Garbe-Schönberg D., Veter M., Stoll B., Weis U., Weber M., Lugli F., Jentzen A., Schiebel R., Wassenburg J.A., Jacob D.E. and Haug G.H. (2019)**

Nano-powdered calcium carbonate reference materials: Significant progress for microanalysis? *Geostandards and Geoanalytical Research*, 43, 595–609.

**Jochum K.P., Nohl U., Herwig K., Lammel E., Stoll B. and Hofmann A.W. (2005)**

GeoReM: A new geochemical database for reference materials and isotopic standards. *Geostandards Geoanalytical Research*, 29, 333–338.

**Jochum K.P., Scholz D., Stoll B., Weis U., Wilson S.A., Yang Q., Schwab A., Börner N., Jacob D.E. and Andreae M.O. (2012)**

Accurate trace element analysis of speleothems and biogenic calcium carbonates by LA-ICP-MS. *Chemical Geology*, 318–319, 31–44.

**Jochum K.P., Stoll B., Herwig K. and Willbold M. (2007)**

Validation of LA-ICP-MS trace element analysis of geological glasses using a new solid-state 193 nm Nd: YAG laser and matrix-matched calibration. *Journal of Analytical Atomic Spectrometry*, 22, 112–121.

**Jochum K.P., Weis U., Stoll B., Kuzmin D., Yang Q., Raczek I., Jacob D.E., Stracke A., Birbaum K., Frick D.A., Günther D. and Enzweiler J. (2011)**

Determination of reference values for NIST SRM 610–617 glasses following ISO guidelines. *Geostandards and Geoanalytical Research*, 35, 397–429.

**Johnstone H.J.H., Steinke S., Kuhnert H., Bickert T., Pälke H. and Mohtadi M. (2016)**

Automated cleaning of foraminifera shells before Mg/Ca analysis using a pipette robot. *Geochemistry Geophysics Geosystems*, 420, 3502–3511.

**Lončarić N., van Iperen J., Kroon D. and Brummer G.-J.-A. (2007)**

Seasonal export and sediment preservation of diatomaceous, foraminiferal and organic matter mass fluxes in a trophic gradient across the SE Atlantic. *Progress in Oceanography*, 73, 27–59.

**Lugli F., Weber M., Giovanardi T., Arrighi S., Bortolini E., Figus C., Cipriani A. (2020)**

Fast offline data reduction of laser ablation MC-ICP-MS Sr isotope measurements via an interactive Excel-based spreadsheet 'SrDR'. *Journal of Analytical Atomic Spectrometry*, 35, 852–862.

**Marchitto T.M. (2006)**

Precise multielemental ratios in small foraminiferal samples determined by sector field ICP-MS. *Geochemistry Geophysics Geosystems*, 7, 1–10.

**McArthur J., Howarth R.J. and Shields G.A. (2012)**

Strontium isotope stratigraphy. In: Gradstein F.M., Ogg J.G.,

Schmitz M. and Ogg G. (eds), *The Geological Time Scale*. Elsevier, 127–144.

**Mischel S.A., Mertz-Kraus R., Jochum K.P. and Scholz D. (2017)**

TERMITE: An R script for fast reduction of laser ablation inductively coupled plasma-mass spectrometry data and its application to trace element measurements. *Rapid Communications in Mass Spectrometry*, 31, 1079–1087.

**Nürnberg D., Bijma J. and Hemleben C. (1996)**

Assessing the reliability of magnesium in foraminiferal calcite as a proxy for water mass temperatures. *Geochimica et Cosmochimica Acta*, 60, 803–814.

**Ohno T. and Hirata T. (2007)**

Simultaneous determination of mass-dependent isotopic fractionation and radiogenic isotope variation of strontium in geochemical samples by multiple collector-ICP-mass spectrometry. *Analytical Sciences*, 11, 1275–1280.

**Okai T., Suzuki A., Kawahata H., Terashima S. and Imai N. (2002)**

Preparation of a new Geological Survey of Japan, geochemical reference material: Coral JcP-1. *Geostandards Newsletter: The Journal of Geostandards and Geoanalysis*, 26, 95–99.

**Palmer M.R. and Edmond J.M. (1992)**

Controls over the strontium isotope composition of river water. *Geochimica et Cosmochimica Acta*, 56, 2099–2111.

**Phillis C., Ostrach D., Ingram B. and Weber P. (2011)**

Evaluating otolith Sr/Ca as a tool for reconstructing estuarine habitat use. *Canadian Journal of Fisheries and Aquatic Sciences*, 68, 360–373.

**Pracht H., Metcalfe B. and Peeters F.J.C. (2019)**

Oxygen isotope composition of the final chamber of planktic foraminifera provides evidence of vertical migration and depth-integrated growth. *Biogeosciences*, 16, 643–661.

**R Core Team (2020)**

R: A language and environment for statistical computing. R Foundation for Statistical Computing (Vienna). <https://www.R-project.org/>

**Swart P.K., Burns S.J. and Leder J.J. (1991)**

Fractionation of the stable isotopes of oxygen and carbon in carbon dioxide during the reaction of calcite with phosphoric acid as a function of temperature and technique. *Chemical Geology*, 86, 89–96.

**Sylvester P.J. (2008)**

Matrix effects in laser ablation-ICP-MS. In: Sylvester P.J. (ed.), *Laser ablation ICP-MS in the Earth sciences: Current practices and outstanding issues*. Mineralogical Association of Canada, Short Course Series, 40, 67–78.

**Tang G.-Q., Li X.-H., Li Q.-L., Liu Y.U. and Ling X.-X. (2019)**

A new Chinese national reference material (GBW04481) for calcite oxygen and carbon isotopic microanalysis. *Surface and Interface Analysis*, 52, 190–196.

## references

**Tarique M., Rahaman W., Fousiya A., Lathika N., Thamban M., Achyuthan H. and Misra S. (2021)**  
Surface pH Record (1990–2013) of the Arabian Sea from boron isotopes of lakshadweep corals – Trend, variability, and control. *Journal of Geophysical Research: Biogeosciences*, 126, 1990–2013.

**Taylor R., Ishizuka O., Michalik A., Milton J.A. and Croudace I. (2014)**  
Evaluating the precision of Pb isotope measurement by mass spectrometry. *Journal of Analytical Atomic Spectrometry*, 30, 198–213.

**Titelboim D., Sadekov A., Hyams-Kaphzan O., Almogi-Labin A., Herut B., Kucera M. and Abramovich S. (2018)**  
Foraminiferal single chamber analyses of heavy metals as a tool for monitoring permanent and short term anthropogenic footprints. *Marine Pollution Bulletin*, 126, 65–71.

**Todd E., Stracke A. and Scherer E.E. (2015)**  
Effects of simple acid leaching of crushed and powdered geological materials on high-precision Pb isotope analyses. *Geochemistry Geophysics Geosystems*, 16, 2276–2302.

**Weber M., Lugli F., Hattendorf B., Scholz D., Mertz-Kraus R., Guinoiseau D. and Jochum K.P. (2020a)**  
NanoSr – A new carbonate microanalytical reference material for *in situ* strontium isotope analysis. *Geostandards and Geoanalytical Research*, 44, 69–83.

**Weber M., Tacail T., Lugli F., Clauss M., Weber K., Leichter J., Winkler D.E., Mertz-Kraus R. and Tütken T. (2020b)**  
Strontium uptake and intra-population  $^{87}\text{Sr}/^{86}\text{Sr}$  variability of bones and teeth – Controlled feeding experiments with rodents (*Rattus norvegicus*, *Cavia porcellus*). *Frontiers in Ecology and Evolution*, 8, 569940.

**Weber K., Weber M., Menneken M., Kral A.G., Mertz-Kraus R., Geisler T., Vogl J. and Tütken T. (2021a)**  
Diagenetic stability of non-traditional stable isotope systems (Ca, Sr, Mg, Zn) in teeth – An *in-vitro* alteration experiment of biogenic apatite in isotopically enriched tracer solution. *Chemical Geology*, 572, 120196.

**Weber M., Hinz Y., Schöne B.R., Jochum K.P., Hoffmann D., Spötl C., Riechelmann D.F.C. and Scholz D. (2021b)**  
Opposite trends in Holocene speleothem proxy records from two neighboring caves in Germany: A multi-proxy evaluation. *Frontiers in Earth Science*, 9, 154.

**Weber M., Lugli F., Jochum K.P., Cipriani A. and Scholz D. (2018)**  
Calcium carbonate and phosphate reference materials for monitoring bulk and microanalytical determination of Sr isotopes. *Geostandards and Geoanalytical Research*, 42, 77–89.

**Willmes M., Glessner J., Carleton S., Gerrity P. and Hobbs J. (2016)**  
 $^{87}\text{Sr}/^{86}\text{Sr}$  isotope ratio analysis by laser ablation MC-ICP-MS in scales, spines, and fin rays as a non-lethal alternative to otoliths for reconstructing fish life history. *Canadian Journal of Fisheries and Aquatic Sciences*, 73, 1852–1860.

**Yu J., Day J., Greaves M. and Elderfield H. (2005)**  
Determination of multiple element/calcium ratios in foraminiferal calcite by quadrupole ICP-MS. *Geochemistry, Geophysics, Geosystems*, 6, 2005GC000964.

**Zachos J., Pagani M., Sloan L., Thomas E. and Billups K. (2001)**  
Trends, rhythms, and aberrations in global climate 65 Ma to present. *Science*, 292, 686–693.

## Supporting information

The following supporting information may be found in the online version of this article:

Table S1.  $\delta^{13}\text{C}_{\text{VPDB}}$  and  $\delta^{18}\text{O}_{\text{VPDB}}$  of NFHS-2-NP obtained from five laboratories (Labs 1B, 3C, 9B, 11 and 12).

Table S2. Mass fractions of NFHS-2-NP obtained from seven laboratories (Labs 1–7).

Table S3. Comparison of total digestion and  $\text{HNO}_3$  dissolution by NIOZ (Lab 3A).

Table S4. Mass fractions and RSD values obtained from analyses NFHS-2-NP measured by NIOZ (Lab 3B) and JGU (Lab 7A) compared with USGS MACS-3, MACS-3 NP, JCP-1 NP and JCt-1 NP.

Table S5.  $^{87}\text{Sr}/^{86}\text{Sr}$  isotope ratio measurement results obtained from four laboratories (Labs 7B, 7C, 8, 9A, 10).

Table S6. Individual  $^{87}\text{Sr}/^{86}\text{Sr}$  isotopes ratios obtained from four laboratories (Labs 7B, 7C, 8, 9A, 10).

Table S7. Example of the B/Ca ratio measurement results from a homogeneity test on a single nano-pellet.

Table S8. Example of a homogeneity test with calculations according to ASTM Guide E826-14 (2014).

Appendix S1. Product information sheet for reference material NFHS-2-NP.

This material is available from: <http://onlinelibrary.wiley.com/doi/10.1111/ggr.12425/abstract> (This link will take you to the article abstract).



## Appendix A

### Data evaluation of pellet homogeneity

#### Homogeneity testing of solid samples using LA-ICP-MS

The homogeneity testing of solid candidate RMs is less straightforward than that of powdered materials. ASTM Guide E826-14 (2014) (<https://www.astm.org/Standards/E826.htm>) provides guidance on this issue. The guide states that the sample surface should be divided into zones in which repeated measurements should be performed. The problem is that the measurements are supposed to be performed on exactly the same spot. This is not possible for typical LA-ICP-MS analyses. An adaptation of the guide's approach is shown in Figure 2 (Materials and methods section). The circle in Figure 2 represents the pellet's sample surface and shows its subdivision into seven analytical zones in which three spot-measurements in the closest feasible proximity to one another should be performed. In total, this yields twenty-one analyses. Each run should be bracketed by

a suitable RM for drift correction, ensuring that any observed variation can be linked to sample composition and not instrumental error. Additionally, the analyses should be carried out in random order by generating three randomised sequences from 1 to 7. Ideally, this procedure should be carried out on several pellets. Traditionally, and following ISO guidelines the number of units required for a homogeneity test can be calculated using Equation (A1):

$$\text{No of units}_{\text{Homogeneity Study}} = \sqrt[3]{\text{Number of produced units}} \quad (\text{A1})$$

An example of B/Ca ratio [ $\text{mmol mol}^{-1}$ ] results from a homogeneity test on a single nano-pellet is shown in Table S7. It shows the means and RSD both within and between the zones. Another example of calculations according to ASTM Guide E826-14 (2014) is shown in Table S8. The highlighted box in green shows a passed homogeneity test. The test passes if the absolute difference of  $t'$  is less than the  $w$  value.